Solar hydrogen for high capacity, dispatchable, long-distance energy transmission - A case study for injection in the Greenstream natural gas pipeline

Energy Conversion and Management 273 (2022) 116398

Contents lists available at ScienceDirect

Energy Conversion and Management

journal homepage: www.elsevier.com/locate/enconman

Solar hydrogen for high capacity, dispatchable, long-distance energy transmission – A case study for injection in the Greenstream natural gas pipeline

Tubagus Aryandi Gunawan [a], Marco Cavana [b], Pierluigi Leone [b], Rory F.D. Monaghan [c,d,e,*]

[a] Andlinger Center for Energy and the Environment, Princeton University, NJ, USA
[b] Department of Energy "Galileo Ferraris", Politecnico di Torino, Torino, Italy
[c] School of Engineering, University of Galway, Ireland
[d] Ryan Institute for Marine, Environmental and Energy Research, Galway, Ireland
[e] MaREI, the SFI Research Centre for Energy, Climate and Marine, Galway, Ireland

ARTICLE INFO

Keywords:
Renewable hydrogen
Hydrogen energy system
Solar energy
Hydrogen injection
Gas transmission

ABSTRACT

This paper presents the results of techno-economic modelling for hydrogen production from a photovoltaic battery electrolyser system (PBES) for injection into a natural gas transmission line. Mellitah in Libya, connected to Gela in Italy by the Greenstream subsea gas transmission line, is selected as the location for a case study. The PBES includes photovoltaic (PV) arrays, battery, electrolyser, hydrogen compressor, and large-scale hydrogen storage to maintain constant hydrogen volume fraction in the pipeline. Two PBES configurations with different large-scale storage methods are evaluated: $PBES_C$ with compressed hydrogen stored in buried pipes, and $PBES_L$ with liquefied hydrogen stored in spherical tanks. Simulated hourly PV electricity generation is used to calculate the specific hourly capacity factor of a hypothetical PV array in Mellitah. This capacity factor is then used with different PV sizes for sizing the PBES. The levelised cost of delivered hydrogen ($LCOH_D$) is used as the key techno-economic parameter to optimise the size of the PBES by equipment sizing. The costs of all equipment, except the PV array and batteries, are made to be a function of electrolyser size. The equipment sizes are deemed optimal if PBES meets hydrogen demand at the minimum $LCOH_D$. The techno-economic performance of the PBES is evaluated for four scenarios of fixed and constant hydrogen volume fraction targets in the pipeline: 5%, 10%, 15%, and 20%. The PBES can produce up to 106 kilotonnes of hydrogen per year to meet the 20% target at an $LCOH_D$ of 3.69 €/kg for compressed hydrogen storage ($PBES_C$) and 2.81 €/kg for liquid hydrogen storage ($PBES_L$). Storing liquid hydrogen at large-scale is significantly cheaper than gaseous hydrogen, even with the inclusion of a significantly larger PV array that is required to supply additional electrcitiy for liquefaction.

1. Introduction

The European Union (EU) aims by 2030 to install 40 GW of electrolyser capacity within its member states and a further 40 GW in neighbouring regions, specifically North Africa and Ukraine, to supply the EU with renewable, or green, hydrogen [1]. Large scale of electrolysers at wind and solar production sites can potentially generate low-carbon hydrogen at levelised production costs as low as 1.5 to 2.0 €/kg by 2025 [2]. The hydrogen produced in these neighbouring regions can be transmitted to the EU via existing natural gas transmission infrastucture. North African countries, including Algeria and Libya, currently provide 24 billion cubic meters (bcm) of natural gas to the EU, equivalent to 5% of total natural gas consumed in the bloc in 2019 [3].

1.1. Hydrogen production using solar energy for dispatchable and standalone operation

Currently, renewable electricity can be commercially generated from solar energy through photovoltaic (PV) and concentrated solar power (CSP) technologies. The global average levelised cost of electricity (LCOE) for PV and CSP in 2020 are 57 and 108 USD/MWh, respectively [4]. The global average installed system cost for utility-scale PV systems is 883 USD/kW [4]. A wide range of studies estimate the costs of solar electricity can be reduced due to the expected continuation of the historic trend of decreasing capital expenditure (CAPEX) of PV in the future

* Corresponding author.
E-mail addresses: arya.gunawan@princeton.edu (T.A. Gunawan), rory.monaghan@universityofgalway.ie (R.F.D. Monaghan).

https://doi.org/10.1016/j.enconman.2022.116398
Received 6 July 2022; Received in revised form 6 October 2022; Accepted 22 October 2022
Available online 8 November 2022

Abbreviations

c	Specific cost, €/kWh or €/kW
C	Total cost, €
E	Energy, kWh
$\dot{E}$	Energy, MWh
$LCOE$	Levelised cost of electricity, €/kWh
$LCOH_D$	Levelised cost of delivered hydrogen, €/kg
LHV	Lower heating value, kWh/kg
M	Mass, kg
$\dot{M}$	Mass flow rate, tonne per day
P	Nominal power, kW_e
$\dot{P}$	Nominal power, MW_e
p	Pressure, barg
r	Discount rate, %
t	Time, hour
T	Time, year

Greek symbols

λ	Capacity factor, %
η	Efficiency, %
τ	Economic lifetime, year
μ	Specific energy consumption, kWh/kg

Subscripts and superscripts

CAPEX	Capital expenditure
CSP	Concentrated solar power
EB	Battery
EC	Electric compressor
EU	European Union
EU-PVGIS	European Union Photovoltaic Geographical Information System
EUMETSAT	European Organisation for the Exploitation of Meteorological Satellites
EMU	Energy management unit
ENG	Engineering
ENTSOG	European Network of Transmission System Operators for Gas
H_2	Hydrogen gas
H_2O	Water
HD	Hydrogen demand
HHV	Higher heating value
HP	Hydrogen production
ICS	Interconnection, commissioning, and start-up
LHV	Lower heating value
LOHC	Liquid organic hydrogen carriers
LS	Large-scale hydrogen storage
LU	Liquefaction unit
MED	Multiple-effect desalination
MENA	Middle East and North Africa
NASA	National Aeronauticsand Space Administration
OPEX	Operation and maintenance expenditure
OH	Other expenditure
OM	Operation & maintenance
PBES	Photovoltaic battery electrolyser system
PV	Photovoltaic
PVT	PV Performance tool
SARAH	Surface Solar Radiation Data Set - Heliosat
SR	Electrolyser stack replacement
SWRO	Seawater reverse osmosis
WE	Water electrolyser

[5–7]. If the CAPEX of PV reaches 458 USD/kW in 2030, the LCOE of PV could be 0.023 to 0.028 USD/kWh [7].

Hydrogen can be produced using PV electricity via a water electrolyser system. In most studies for a standalone system, solar hydrogen is employed as storable energy carrier for a fuel cell to regenerate electricity. When PV is integrated with hydrogen and battery, modelling work by Kikuchi et. al. found that the addition of a battery to the hydrogen production from PV electricity can improve the productivity of the electrolyser [8]. Battery and hydrogen can play important roles to level the intermittent of solar energy and loads [9]. Even though Burhan et al. found that a PV-hydrogen system without the aid of battery can produce electricity that meets the daily loads [10], Castañeda et al. showed that the PV-hydrogen only system can be more expensive compared to PV-battery only system [11]. The PV-battery-hydrogen modelling by Xie et al. found that storing PV electricity in the form of hydrogen can improve the reliability of power supply as well as reducing the cost of energy [12]. In line with Xie et al., Marocco et al. emphasized the importance of producing hydrogen for long-term storage to increase system capability to deliver electricity throughout the year [13]. The study also found another role of hydrogen, which is to prevent oversizing the PV arrays and battery. According to a study by Mah et al., there is a potential waste of solar energy from oversized PV arrays that is typically aimed to reduce energy storage capacity [14]. Most literature on PV-battery-hydrogen systems for standalone operation are for relatively small capacities to meet the electricity demand for off-grid communities and buildings.

Studies of large PV-battery-hydrogen systems are mostly for grid connected applications. A study by Dispenza et. al [15] found that the addition of a battery can store excess PV electricity to be used by the electrolyser later, for example at night. Thus, the battery can reduce grid electricity usage as well as the carbon intensity of hydrogen production. When considering the variability of electricity prices, Coppitters et al. found that a PV-battery-hydrogen design offers a cost-effective alternative while reducing the possibility of electricity supply failure, such as blackout, compared to a system entirely dependent on grid electricity [16]. At another study, Cerchio et al. modelled a large scale PV-hydrogen system to minimise the operational costs under price variation over time [17]. For a large-scale hydrogen production system, the study recommends evaluation of water availability and large-scale hydrogen storage rigorously. According to another study by Zhang et al., optimisation of hydrogen storage size can improve the operation efficiency and net-present values of the system during seasonal mismatch between load and demand [18].

1.2. High capacity, long term hydrogen storage

An extensive review of large-scale storage techniques of hydrogen by Andersson et al. described that hydrogen can be feasibly stored at significant quantity via (1) chemical storage with metal or chemical hydrides, (2) physical storage in the form of compressed or liquid hydrogen, and (3) adsorption via porous carbon-based, porous polymeric, or metal–organic materials [19]. Most techno-economic modelling works explore the chemical and physical storage techniquess due to their near-term potentials. For large-scale chemical storage, Kavadias et al. modelled the techno-economic perfromance of metal-hydride to store hydrogen [20]. The study found that metal-hydride hydrogen storage enables more renewable energy penetration for sites with limited available land on multiple islands in Aegean Sea. In another study, Farag et al. modelled the opportunity of storing hydrogen in the form of liquid organic hydrogen carrier (LOHC) [21]. This study found that the costs of producing hydrogen from grid electricity, converting it to LOHC, transport it via trucks, then converting it back to hydrogen to

meet transportation demand for distributed production systems are more economically viable than a centralised one.

For large-scale physical storage, compressed hydrogen gas can be kept in low-pressure buried pipes (less than 60 barg) or high-pressure salt caverns (higher than 60 barg), if locally available [22]. Low pressure storage is the most technically efficient option, due to the high compressor energy consumption that can be avoided [23]. In the United States, Mallapragada et al. found that the use of large-scale hydrogen storage such as salt cavern can minimise hydrogen production and storage costs to around 2 $/kg when the capacity factor of PV is between 22% and 26% [24]. In Germany, Welder et al. investigated the opportunities of producing hydrogen using renewables, transporting it via pipelines, storing hydrogen across multiple underground storage techniques, and delivering it to transportation and industrial demands [25]. All these new pieces of infrastructures cost 9.5 €/kg. Without the use of salt caverns, the study estimated the delivered hydrogen costs would increase by 15%. In terms of storage capacity, a study by Reuß et al. estimated the hydrogen stockpiling at the large-scale hydrogen storages should cover at least 60 days of German nation-wide hydrogen demand for transportation which comprises 18 days of seasonal reserves and 42 days of standby reserves [26]. As investigated by Mah et al., specific regions such as Southeast Asia can have several days to a month without sufficient sunshine to cost-effectively produce hydrogen from PV [27]. This leads to higher overall costs of hydrogen production using solar electricity solely, which is mainly due to the requirements for larger electrolyser, battery and hydrogen storage. When large-scale geological hydrogen storage is paired with electrical grid infrastructures, Elberry et al found the storable energy in the form of hydrogen enables seasonal storage for renewables to meet the electricity demand in Finland [28]. This is due to the fact that electricity can be rapidly supplied by fuel cells using storable hydrogen mostly produced from surplus renewables. The use of large-scale storage of hydrogen to provide electricity via hydrogen fuelled compressed air energy storage also has been investigated by O'Dwyer et al. [29]. For a system in which hydrogen also needs to satisfy heat demand, Samsatli et al. sized the required underground storage capacities according to the variety of heat demands throughout the year. The study showed the significant increase of heat needed to be satisfied by electricity if large-capacity hydrogen storage is not built, which would eventually lead to a higher-cost system [30]. Other than underground storage, an evaluation by Quarton et al. also considered the storage of hydrogen in gas distribution and transmission linepacks, in which hydrogen that can be stored in the pipeline itself, mostly used to cover demand variation in short time [31]. In another study, Seo et al. investigated the opportunity of storing hydrogen from multiple energy resources and sites in a centralised large-capacity hydrogen storage facility. By gaining the impact of economies of scale, the overall costs of delivering hydrogen for transport sector can be less at centralised storage sites compared to distributed ones [32]. A study by Gabrielli et al. also suggested the use of underground storage for large-scale hydrogen system when available [33]. The study found that the integrated short-term storage by battery and long-term storage by salt cavern can significantly reduce CO_2 emissions while synchronising the energy supply–demand mismatch. Such a system requires significantly larger hydrogen storage than electricity storage. However, the salt caverns required for this type of geological storage are not available at every location.

In liquid form, hydrogen can be stored in spherical tanks [34]. A comprehensive review of hydrogen liquefaction by Aasadnia et al. [35] and Ghorbani et al. [36] showed various energy sources from natural gas to solar energy can be used to power the hydrogen liquefaction, multiple liquefaction cycles, numerous different equipment configuration, and wide-ranges of capacities between 100 and 290 tonnes per day (TPD). The study estimated the specific energy consumption for hydrogen liquefaction is in the range of 4 to 15 kWh/kg. Several studies by Cardella et al. [37,38] showed the significant scale up of hydrogen liquefaction processes from 5 tonnes per day (TPD) to a 100-TPD liquefaction plant can deliver cost reduction up to nearly 70%.

1.3. Long-distance hydrogen transportation

For large capacity and long distance, hydrogen can be transported via pipeline in pure form or blended with natural gas. In pure form, a study by Saadi et al. found that delivering costs ($/MWh) of hydrogen gas through pipelines can be significantly higher than delivering other chemical-based energy carriers like oil and natural gas [39]. However, according to the findings of Miao et al, producing hydrogen then transporting it in pure form via large capacity onshore pipelines (5,000 MW) over long distances (1,000 to 10,000 km) is less expensive compared to transporting electricity via onshore cable then producing the same amount of hydrogen [40]. Offshore hydrogen pipelines are more cost effective than electrical cables when the transmission capacity is at least 1,000 MW. In another study, Demir et al. found the costs of delivering hydrogen onshore via a new build large-scale dedicated pipeline network can be as low as 2 €/kg [41]. Large-scale storage facilities and transmission pipelines for hydrogen are essential technologies for the future hydrogen deployment at scale [42,43].

Hydrogen delivery costs can be minimized by utilizing the existing energy infrastructure. Existing onshore or offshore natural gas pipelines are investigated by multiple studies to deliver hydrogen in the mixture of natural gas. A detailed review by Messaoudani et al. listed the safely considerations for blending hydrogen with natural gas [44]. In the distribution level, a study by Liu et al. [44] and Li et al. [45] evaluated blending strategies to manage pressure drop and temperature drop in the pipelines, respectively. The results of modelling work by Pellegrino et al. showed that the operational strategies of gas networks need to be adjusted, i.e. in compression and regulation stations, after blending hydrogen [46]. In the production level, a study by Mukherjee et al. investigated the opportunity to produce hydrogen during low electricity price periods then injected it into existing natural gas pipelines. The study found that hydrogen blending can reduce CO_2 emissions which provides an opportunity to capture more revenues from emission reduction credits of 15 $/t$CO_2$ reduced in Alberta, Canada [47]. For hydrogen from wind energy, Gunawan et al. modelled the distributed hydrogen production from curtailed wind electricity at existing wind farms in Ireland for injection at the existing natural gas network. The study found that the future cost of distributed production and transportation of hydrogen to the nearest injection locations is 6–8 €/kg [48]. For hydrogen from solar energy, Cavana et. al. investigated the technical challenges of injecting and blending different volume fractions of hydrogen produced from PV electricity into a long-distance gas transmission pipeline [49]. The study found that there are multiple mismatches between hydrogen supply and demand capacities due to fact that hydrogen production relies on solar energy, which leads to the need of large-scale energy storage.

1.4. Contributions, objectives & outline of the paper

The literature review shows that most of the studied standalone solar hydrogen production and storage systems are at relatively small capacity and designed to supply hydrogen to meet electricity, heat, and transport demands. Most large-scale storage techniques for hydrogen are widely studied for underground storages. Underground storage, the most cost-effective form of hydrogen storage, is frequently not located in the same region as renewable resources. This provides the opportunity to assess liquid hydrogen in spherical tanks as large-scale hydrogen storage. In addition, there is a lack of literature that evaluates the potential of buried pipes to store gaseous hydrogen as another possible low-cost, large-capacity storage option. In terms of transporting hydrogen in the existing natural gas transmission pipeline, the available studies have not evaluated the economical aspects of providing solar hydrogen for blending and not exploited the potential of adding battery storage to improve the reliability of energy management for hydrogen

production and storage. In summary, there are research gaps in (1) large-scale PV-battery-hydrogen for standalone operation, (2) renewable hydrogen production system that is integrated with large-scale spherical tanks and buried pipes, and (3) techno-economic evaluation of supplying solar hydrogen at a large-scale for the existing large-capacity and long-distance natural gas transmission pipeline. This study contributes to the state of the art by developing a techno-economic modelling method to design a cost-effective and large-scale PV-battery-hydrogen system that is assisted either by compressed or liquefied hydrogen storage to meet multiple hypothetical hydrogen demands imposed by a long-distance natural gas transmission pipeline. The objectives of this study are (1) to design and model hydrogen supply from a photovoltaic battery electrolyser system (PBES) with either compressed ($PBES_C$) or liquefied hydrogen storage ($PBES_L$), (2) to evaluate the impact on hydrogen delivery costs for different equipment size combinations, and (3) to determine the optimal equipment sizes of the PBES that meets specific hydrogen demand at the lowest cost. The following section describes the methods used to model the techno economic performance of the PBES. Following that, the results and discussion section comprises the description of the techno-economic performance for PV arrays, battery, electrolyser, and storage, the optimum equipment sizes for all scenarios, hydrogen supply from the optimum equipment, energy and water intensities of hydrogen supply, and sensitivity analysis. Finally, the overall findings of the work and impacts on the hydrogen production and storage system are presented in the conclusions section.

2. Methods

2.1. Systems & scenarios

Hydrogen can potentially be generated using a photovoltaic battery electrolyser system (PBES) in a region with high solar energy potential like North Africa. As a case study, this work models renewable hydrogen production from solar energy in North Africa and its injection into the existing subsea gas transmission pipeline between Libya and Italy. The hydrogen is assumed to be produced and injected at the Mellitah Gas Compression Station (MGCS) in Libya, transported through the 520-km Greenstream subsea natural gas transmission pipeline and delivered to the Gela receiving terminal in Italy, as shown in Fig. 1. In the PBES, electricity is generated by photovoltaic (PV) arrays. The model to calculate the PV electricity is explained in the next subsection. The PBES is evaluated with two different configurations of large-scale hydrogen storage: compressed hydrogen in buried pipes ($PBES_C$), and liquefied hydrogen in spherical tanks ($PBES_L$). The parameters of these storage configurations are described in the subsection on large-scale hydrogen storage. The PV electricity can be stored over short durations in a battery system and/or used to produce hydrogen via water electrolysis in the PBES as illustrated in Fig. 2. In the $PBES_L$ configuration, electricity is additionally needed for the hydrogen liquefaction, as shown in Fig. 2.b. In both, configurations, when it is required, hydrogen is compressed to 80 barg for injection to the gas transmission pipeline. Hydrogen production is modelled to meet the hourly demand required by hydrogen volume fractions of 5%, 10%, 15% and 20% in the Greenstreram pipeline, which is explained in hydrogen demand subsection.

2.2. Photovoltaic electricity

PV electricity production for the coordinates of Mellitah, Libya is simulated using the PV Performance tool (PVT) from the European Union Photovoltaic Geographical Information System (EU-PVGIS) [51]. The solar radiation database collected by the Surface Solar Radiation Data Set - Heliosat (SARAH) and recorded by the European Organisation for the Exploitation of Meteorological Satellites (EUMETSAT) Climate Monitoring Satellite Application Facility (CM SAF) from 2005 to 2015 are used in the simulation. PVT optimises the slope and azimuth of the fixed mounting PV arrays in the simulation of PV electricity. The PV technology, installed nominal power PV power for slope and azimuth optimisation only (P_{PVT}), and system losses are crystalline silicon, 1,000 kW_e, and 14%, respectively. The average hourly PV electricity from PVT (E_{PVT}) is then calculated from these ten years of data. The PV capacity factor as a function of time t ($\lambda_{PV,t}$) can be calculated using Equation (1). Hourly PV electricity production (E_{PV}) for different array sizes (P_{PV}) at PBES can be calculated using Equation (2).

$$\lambda_{PV,t} = \frac{E_{PVT,t}}{P_{PVT} \times \Delta t} \tag{1}$$

$$E_{PV,t} = P_{PV} \times \lambda_{PV,t} \times \Delta t \tag{2}$$

2.3. Large-scale storage of compressed and liquefied hydrogen

As described in Subsection 1.2, large-scale hydrogen can be stored in the forms of compressed gas and liquid. In gas form, hydrogen storage in salt caverns is cheaper than buried [52], however, due to the relative lack of salt deposits in Libya [53,54], buried pipes are assumed to be used in this study for storing compressed hydrogen. The buried pipes are made of thick and low-strength carbon steels, due to high-strength steels are more susceptible to hydrogen embrittlement [55]. When storing hydrogen in liquid form, this study assumes the use of spherical tanks [34]. The energy demand for liquefaction is assumed at 9.3 kWh/kg, which includes all the required conversion steps from 30 barg hydrogen input to 30 barg hydrogen output [56]. The details of each storage technology for a base year of 2030 are given in Table 1. In contrast, there is no additional energy demand for compressed hydrogen storage due to hydrogen output from electrolyser is assumed at 30 barg as shown in Table 2.

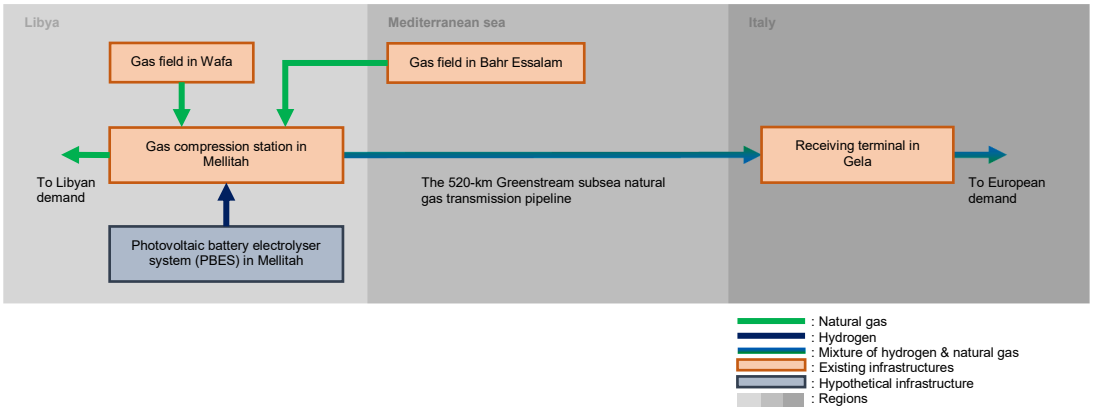

Fig. 1. Mellitah (Libya) and Gela (Italy) gas terminals are connected by the 520-km Greenstream subsea natural gas transmission pipeline (reproduced from [49,50]).

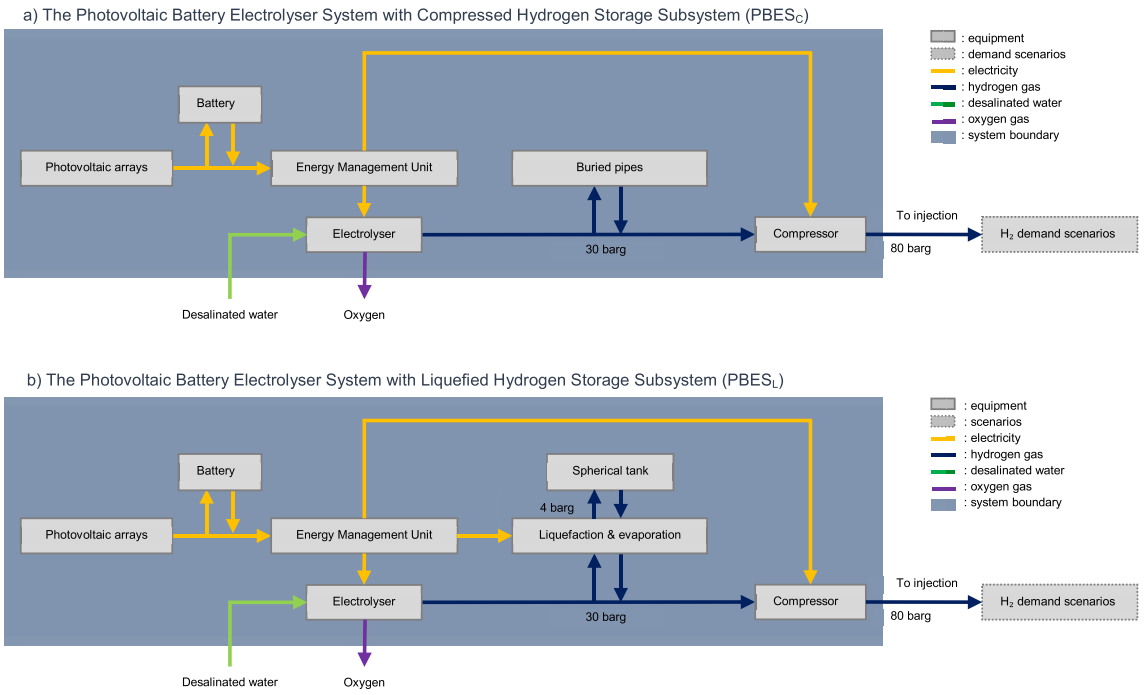

Fig. 2. The components of a photovoltaic battery electrolyser system for hydrogen gas grid injection with (a) compressed hydrogen storage in buried pipes (PBES$_C$), (b) and liquefied hydrogen storage in spherical tank (PBES$_L$).

Table 1
Techno-economic parameters of large-scale hydrogen storages (LS).

Hydrogen forms Technology	Compressed hydrogen Buried pipes			Liquefied hydrogen Spherical tank and liquefaction unit (LU)		
Lifetime, τ	50	years	[22]	30	years	[52]
Working pressure	20–70	barg	[22]	1	barg	[52]
CAPEX, C_{CAPEX}	300 × M_{H2}	€	[22]	7.37 × $\dot{M}_{H2}^{2/3}$	M€	[57]
OPEX, C_{OPEX}	2	%	[22]	10% x C_{CAPEX}	€	[58]
Specific energy consumption, μ_{LU}				(liquefaction) 9.3	kWh/kg	[56]
Hydrogen loss	0.5	%	[43]	(boil-off) 0.01	%	[34]
Stored hydrogen temperature	25	°C	[59]	−252.9	°C	[34]
Stored hydrogen pressure	30	barg	[59]	0.1	barg	[34]
Stored hydrogen density	20.537	kg/m^3	[59]	70.973	kg/m^3	[34]

2.4. Levelised cost of hydrogen

The levelised cost of delivered hydrogen ($LCOH_D$) and annual hydrogen production ($M_{H2,HP}$) are used as the key parameters to optimise the equipment sizes of PBES techno-economically. $LCOH_D$ is calculated from total capital (C_{CAPEX}), operational and maintenance expenditure (C_{OPEX}), and total hydrogen produced ($M_{H2,HP}$) for the year (T) using Equation (3). The PBES lifetime (τ_{PBES}) is defined to operate for 20 years with a discount rate (r) of 5% [60]. Annual hydrogen production ($M_{H2,HP}$) is described in the following subsection on hydrogen supply.

$$LCOH_D = \frac{\sum_{T=0}^{T=\tau_{PBES}} \frac{C_{CAPEX}}{(1+r)^T} + \sum_{T=0}^{T=\tau_{PBES}} \frac{C_{OPEX}}{(1+r)^T}}{\sum_{T=0}^{T=\tau_{PBES}} \frac{M_{H2,HP}}{(1+r)^T}} \quad (3)$$

The C_{CAPEX} includes the capital costs of the PV array (C_{PV}), battery (C_{EB}), water electrolyser (C_{WE}), electric compressor (C_{EC}), large-scale storage (C_{LS}, either buried pipes or cryogenic liquid, depending on the configuration), energy management unit (C_{EMU}), interconnection, commissioning, and start-up (C_{ICS}), engineering (C_{ENG}) and other costs (C_{OH}), as expressed by Equation (4). The hydrogen injection system is not considered due to the limitation of publicly available data and relatively low of cost share. The C_{OPEX} comprises the operational and maintenance costs of PV arrays ($C_{OM,PV}$), water electrolyser ($C_{OM,WE}$), electric compressor ($C_{OM,EC}$), and large-scale storage ($C_{OM,\ LS}$), as well as the stack replacement (C_{SR}) and water consumption (C_{H2O}) as shown by Equation (5). All the costs are made to be a function of electrolyser size (P_{WE}), except for PV, battery, and hydrogen storage costs, which are independent variables. Capital costs for electrolyser and batteries are projected to decrease by 50% and 60%, respectively, between 2020 and 2030[61 8]. All techno-economic parameters for the PBES constituent equipment for a commencement year of 2030 are listed in Table 1.

$$C_{CAPEX,HP} = C_{PV} + C_{EB} + C_{WE} + C_{EC} + C_{LS} + C_{EMU} + C_{ICS} + C_{ENG} + C_{OH} \quad (4)$$

$$C_{OPEX,HP} = C_{OM,\ PV} + C_{OM,\ WE} + C_{OM,EC} + C_{OM,LS} + C_{SR} + C_{H2O} \quad (5)$$

2.5. Hydrogen supply

Annual hydrogen production ($M_{H2,HP}$) is calculated from the electricity (E_{WE}) used by the electrolyser and its specific electricity consumption (μ_{WE}) as expressed in Equation (6) [48]. The electrolyser operates with electricity from the PV array ($E_{PV,WE}$) and battery ($E_{EB,WE}$),

Table 2
Techno-economic parameters of hydrogen production in a photovoltaic battery electrolyser system.

Parameters, Symbol	Value/ Unit/ Reference					
Equipment	**Water Electrolyser (WE)**			**Electric Compressor (EC)**		
Technology	Alkaline			Reciprocating		
Sp. energy cons., μ	48	kWh/kg	[56]	0.7	kWh/kg	[62]
Lifetime, τ	20 (system), 11 (stack)	years	[63]	10	years	[62]
Efficiency, η	69%	(LHV_{H2})	[62]	73%	isentropic	[64]
Outlet pressure, p	30	barg	[62]	80	barg	[65]
CAPEX, C_{CAPEX}	$3645 \times P_{WE}{}^{0.783}$	€	[66]	$4342 \times P_{WE,n}{}^{0.66}$	€	[67]
OPEX, C_{OPEX}	$0.2011\ P_{WE,n}{}^{-0.23} \times C_{CAPEX,WE}$	€	[62 61]	2%	of *CAPEX*	[62]
ICS	20% x ($C_{WE} + C_{EC}$)	€	[67]			
Engineering	15% x ($C_{WE} + C_{EC}$)	€	[67]			
Other cost, C_{OH}	$1.5652\ P_{WE,n}{}^{-0.154} \times C_{CAPEX,WE}$	€	[67]			
Stack rep., C_{SR}	$353\ xP_{WE}{}^{0.929}$	€	[63,67]			
Equipment	**Photovoltaic (PV)**			**Energy management unit (EMU)**		
Technology	Polycrystalline silicon			Controller		
Lifetime, τ	30	years	[68]	15	years	[68]
Efficiency, η	10–15%		[51]	90%		[68]
Capacity factor, λ	Calculated using Equation (1) Annual average is 19%					
CAPEX, C_{CAPEX}	$450 \times P_{PV}$	€	[5,7]	10% x ($C_{WE} + C_{EC}$)	€	[67]
OPEX, C_{OM}	1.5%	of *CAPEX*	[8]			
Equipment	**Battery (EB)**					
Technology	Lithium Nickel Manganese Cobalt Oxide					
Lifetime, τ	20	years	[69]			
Efficiency, η	80%	roundtrip	[8]			
DoD	100%		[69]			
C-rate	1C		[69]			
CAPEX, C_{CAPEX}	$3283 \times E_{EB,n}{}^{0.7108}$	€	[70]			
OPEX, C_{OPEX}	Not considered		[8]			

as shown in Equation (7).

$$M_{H2,t} = \frac{E_{WE,t}}{\mu_{WE}} \tag{6}$$

$$E_{WE,t} = E_{PV,WE,t} + E_{EB,WE,t} \tag{7}$$

The modelling of electrolyser and compressor performance is done in the same manner as in Gunawan et. al [48]. There are two conditions to calculate hourly electricity flow from the PV array to the electrolyser. The first is when the PV electricity production (E_{PV}, result of P_{PV} multiplied by time-step) exceeds electrolyser maximum electricity input (E_{WE}, result of electrolyser capacity P_{WE} multiplied by time-step), the PV electricity for electrolyser ($E_{PV,WE,t}$) is equal to maximum electricity input of electrolyser (E_{WE}). It means PV arrays can generate surplus electricity at small electrolyser sizes. This condition is expressed in Equation (8). The surplus electricity over time can be stored in the battery to be used in the second condition, which occurs when E_{PV} is lower than E_{WE}. Equation (9) shows how the hourly flow of battery electricity to electrolyser ($E_{PB,WE,t}$) can be calculated to support hydrogen production when there is enough stored energy in the battery.

$$E_{PV,WE,t} = \min\left(P_{WE}, P_{PV,t}\right) \times \Delta t \tag{8}$$

$$E_{EB,WE,t} = \min\left(E_{WE,t} - E_{PV,WE,t}, E_{WE,t}\right) \tag{9}$$

In the liquefied hydrogen storage configuration, $PBES_L$, electricity for the liquefaction unit (E_{LU}) is supplied by the PV array and battery as expressed in Equation (10). The amount of PV electricity for liquefaction is calculated using the mass of hydrogen to the large-scale storage at time t ($M_{H2,LS,t}$) and the specific electricity consumption of the liquefaction process (μ_{LU}) as shown in Equation (11). When there is not enough PV electricity, battery supplies the rest of electricity demand for liquefaction as shown in Equation (12).

$$E_{LU,t} = E_{PV,LU,t} + E_{EB,LU,t} \tag{10}$$

$$E_{PV,LU,t} = \min\left(M_{H2,LS,t} \times \mu_{LU}, E_{PV,t} - E_{PV,WE,t}\right) \tag{11}$$

$$E_{EB,LU,t} = \min\left(M_{H2,LS,t} \times \mu_{LU}, \left(M_{H2,LS,t} \times \mu_{LU}\right) - E_{PV,LU,t}\right) \tag{12}$$

Like the water electrolyser, the electric compressor is also powered by electricity from the PV array ($E_{PV,EC}$) and battery ($E_{EB,EC}$), as shown in Equation (13). If the PV electricity supply is larger than the electricity demand for an electrolyser and liquefaction unit, the contribution of PV electricity for the compressor can be calculated using Equation (14). The electricity stored in the battery can also be used to operate the compressor when PV electricity is insufficient, as expressed in Equation (15). The electricity demand for compressing hydrogen gas can be calculated from the mass at time t ($M_{H2,(t)}$) and the specific electricity consumption of the compressor (μ_{EC}).

$$E_{EC,t} = E_{PV,EC,t} + E_{EB,EC,t} \tag{13}$$

$$E_{PV,EC,t} = \min\left(M_{H2,t} \times \mu_{EC}, E_{PV,t} - E_{PV,WE,t} - E_{PV,LU,t}\right) \tag{14}$$

$$E_{EB,EC,t} = \min\left(M_{H2,t} \times \mu_{EC}, \left(M_{H2,t} \times \mu_{EC}\right) - E_{PV,EC,t}\right) \tag{15}$$

The modelling of battery and hydrogen storage performance is done in the same manner as in Ma et. al. [71] and Song et al. [72]. PV electricity charges the battery when its supply exceeds the combined electricity consumption for electrolyser, liquefaction unit, and compressor. The energy stored during battery charging can be calculated using Equation (16). Equation (17) shows the calculation of energy stored in the battery during battery discharge to the electrolyser, liquefaction unit, and compressor.

$$E_{EB,t} = E_{EB,t-1} + \left(\left(E_{PV,t} - E_{PV,WE,t} - E_{PV,LU,t} - E_{PV,EC,t}\right) \times \eta_{EB}\right) \tag{16}$$

$$E_{EB,t} = E_{EB,t-1} + \left(\left(E_{EB,WE,t} + E_{EB,LU,t} + E_{EB,EC,t}\right) \times \eta_{EB}\right) \tag{17}$$

In this study, the hydrogen storage meets the hourly hydrogen

injection demand ($M_{H2,HD,(t)}$). Hydrogen is added to storage when its production surpasses the hourly demand expressed in Equation (18). Hydrogen is released from storage when the hourly hydrogen production is less than hydrogen demand and can be calculated using Equation (19). The maximum of all hourly (at time t) stored hydrogen capacities ($M_{H2,LS(t)}$) throughout the year determines the required storage size. In terms of equipment sizing, the $LCOH_D$ calculation is performed iteratively using different equipment sizes with intervals of 5 MW_e for PV arrays, 5 MW_e for electrolyser, and 5 MWh for battery. The range of equipment sizes for each equipment is listed in Table 3. The equipment size combination for the minimum $LCOH_D$ is selected as the optimum system design.

$$M_{H2,LS,t} = M_{H2,LS,t-1} + \left(\left(\frac{E_{PV,WE,t} + E_{EB,WE,t}}{\mu_{WE}} \right) - M_{H2,HD,t} \right) \quad (18)$$

$$M_{H2,LS,t} = M_{H2,LS,t-1} - \min\left(M_{H2,HD,t} - \left(\frac{E_{PV,WE,t} + E_{EB,WE,t}}{\mu_{WE}} \right), M_{H2,HD,t} \right) \quad (19)$$

2.6. Desalinated water supply

Mellitah is chosen as the location for the PBES because (1) it has an existing gas terminal that could potentially be used for hydrogen injection, and (2) it is situated near the Mediterranean coast, which is favourable for water supply from a hypothetical seawater desalination plant. There are at least two desalination technologies to convert seawater to desalinated water, (I) multiple-effect desalination (MED), and (II) seawater reverse osmosis (SWRO). The World Bank reported that the total annualised cost of desalinating seawater from the Mediterranean Sea is 0.57 € per m^3 for MED and 0.39 € per m^3 for SWRO [73]. Energy use for desalination plants in the Middle East and North Africa (MENA) accounts for 10% of total MENA primary energy usage. The typical energy consumption of SWRO is 1.8 kWh per m^3 of desalinated water.

Desalinated water production from seawater using solar energy has been widely investigated in several studies. Palenzuela et. al. modelled the integration of MED and concentrating solar power (CSP) using seawater from the Mediterranean Sea [74]. The study found the levelised cost of water production is between 0.92 and 1.05 €/m^3. In another study, El-Bialy et. al. analysed a wide range of desalination systems using direct solar energy [75]. The study found various techniques to produce desalinated water from brine using passive or active solar stills. These processes have potential for water supply in the future, especially when the capacity and cost of water production are significantly improved from current levels. This study assumes that the water for electrolysis is purchased at a price of 0.39 € per m^3 from a hypothetical SWRO, which is outside the boundary of the current techno-economic assessment.

Table 4
Summary of annual hydrogen demand for all scenarios.

Parameters	Unit	Demand scenarios			
		5%	10%	15%	20%
Annual H_2 demand (mass)	kilotonnes/year	25.47	50.41	77.29	106.24
Annual H_2 demand (volume)	million Sm^3/year	299.56	592.81	908.90	1,249.26

2.7. Hydrogen demand

Hourly data for natural gas flow and calculated hydrogen demand for four hydrogen volume fraction scenarios for the Greenstream transmission pipeline is obtained from Cavana et. al. [49]. These representative scenarios are chosen because the hydrogen suitability studies on natural gas infrastructure items and final users' appliances are carried out within these ranges. According to a report from MARCOGAZ, a technical association of the European gas industry, it is shown that most of the components of the natural gas infrastructure and its value chain are fit for hydrogen blending up to 20% (by volume) [75]. In addition, considering the main gas quality parameters that are regulated in the technical norms all over Europe (i.e. Wobbe Index, Higher Heating Value and Relative Density), the hydrogen addition has the general effect to lower down the value of all these indicators, as they are measured in terms of unit volume in standard or normal condition. In the case of natural gas form North Africa countries, which has generally a higher fraction of butane and propane, the hydrogen share that makes the blend non-compliant with the quality ranges may be between 14% and 16.4% (with reference to the Italian regulation, depending to the gas quality parameter) or as high as 29.8% referring to the Spanish one about Wobbe Index [76]. In this study, the PBES is located in Mellitah to meet the annual hydrogen demands listed in Table 4. Hourly hypothetical hydrogen demand profiles for one week for each of the four scenarios are shown in Fig. 3.

The hydrogen profiles are obtained through the same rationale explained in [49]: starting from the data for real gas flows available on the European Network of Transmission System Operators for Gas

Table 3
The ranges for equipment sizing of photovoltaic battery electrolyser system with compressed ($PBES_C$) and liquefied ($PBES_L$) hydrogen storage.

	Formula		Minimum and maximum values for H_2 injection scenarios			
			5%	10%	15%	20%
Compressed hydrogen storage						
PV array sizes, $\dot{P}_{PV}$ (MW_e)	Min	$=M_{H2}/(\mu_{WE}+\mu_{EB})/(\lambda_{PV}*8760)$	735	1,454	2,229	3,064
	Max	$=\dot{P}_{PV,minimum}/\eta_{EB,roundtrip}$	918	1,817	2,786	3,830
Electrolyser sizes, $\dot{P}_{WE}$ (MW_e)	Min	$=M_{H2}/(\mu_{WE}+\mu_{EB})/8760$	140	276	424	582
	Max	$=\dot{P}_{PV,maximum}$	918	1,817	2,786	3,830
Battery sizes, $\dot{E}_{EB}$ (MWh)	Min	=10	10	10	10	10
	Max	$=\dot{P}_{PV,maximum}$	918	1,817	2,786	3,830
Liquefied hydrogen storage						
PV array sizes, P_{PV} (MW_e)	Min	$=M_{H2}/(\mu_{WE}+\mu_{EB}+\mu_{LU})/(\lambda_{PV}*8760)$	888	1,757	2,694	3,702
	Max	$=\dot{P}_{PV,minimum}/\eta_{EB,roundtrip}$	1,110	2,196	3,367	4,628
Electrolyser sizes, $\dot{P}_{WE}$ (MW_e)	Min	$=M_{H2}/(\mu_{WE}+\mu_{EB}+\mu_{LU})/8760$	169	334	512	703
	Max	$=\dot{P}_{PV,maximum}$	1,110	2,196	3,367	4,628
Battery sizes, $\dot{E}_{EB}$ (MWh)	Min	=10	10	10	10	10
	Max	$=\dot{P}_{PV,maximum}$	1,110	2,196	3,367	4,628

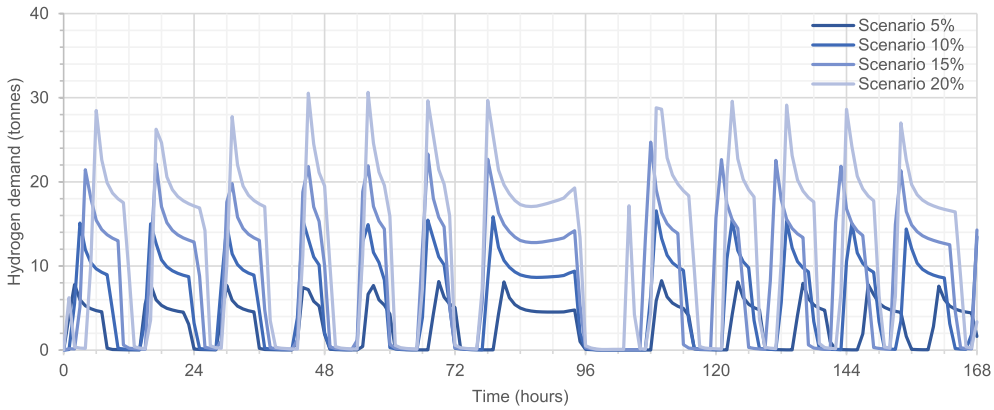

Fig. 3. Hourly hydrogen demand profiles for one representative week for the Greenstream transmission pipeline.

(ENTSOG) Transparency Platform [77] at the gas entry point of Gela in Italy, the hourly hydrogen flow rate delivered to the Italian border has been calculated for each blending scenario to maintain the constant amount of chemical power delivered (evaluated on HHV basis). As the volumetric heating value of the hydrogen is, in this case, 3.25 times smaller than the one of natural gas, the hydrogen volume share contributes to the substitution of a smaller amount of natural gas (as the energy delivered must remain constant), while increasing the volume of the blend.

As the injection point is located upstream the compressor that controls the gas flowing through the Greenstream pipeline, the fluid-dynamic model of the infrastructure presented in [49] is utilised to determine the gas flow at the injection point. This profile is determined by the operational schedule of the compressor station that is, in turn, dependant on the preservation of a minimum pressure threshold at the delivery point. This results in a slightly different gas flow pattern due to the impact of the hydrogen presence within the gas flow which determines a higher volumetric gas flow rate thus higher pressure losses and slightly different compression station operational schedule as visible in Fig. 3.

2.8. Overall model

A photovoltaic battery electrolyser system (PBES) is modelled to produce hydrogen for blending with natural gas. The PBES includes the PV arrays to generate electricity, a battery to temporarily store the electricity when needed, an electrolyser to produce hydrogen, a compressor to compress the hydrogen to 80 barg, and hydrogen storage, either compressed gas in buried pipes or cryogenic liquid in spherical tanks, to maintain the required injection flow rate. The total capital, operational, and maintenance costs and total hydrogen produced PBES during its lifetime are used to calculate the $LCOH_D$. Each combination of equipment sizes results in a specific $LCOH_D$. Therefore, $LCOH_D$ for each injection volume fraction scenario and storage configuration is iteratively calculated using the different equipment size combinations. The set of optimum equipment sizes for a PBES of each storage configuration that meets each injection volume fraction scenario is found at the minimum $LCOH_D$, as illustrated in Fig. 4.

3. Results and discussion

The results of the analysis are discussed into two parts. The first part (section 3.1) seeks to explore the performance of the PBES using

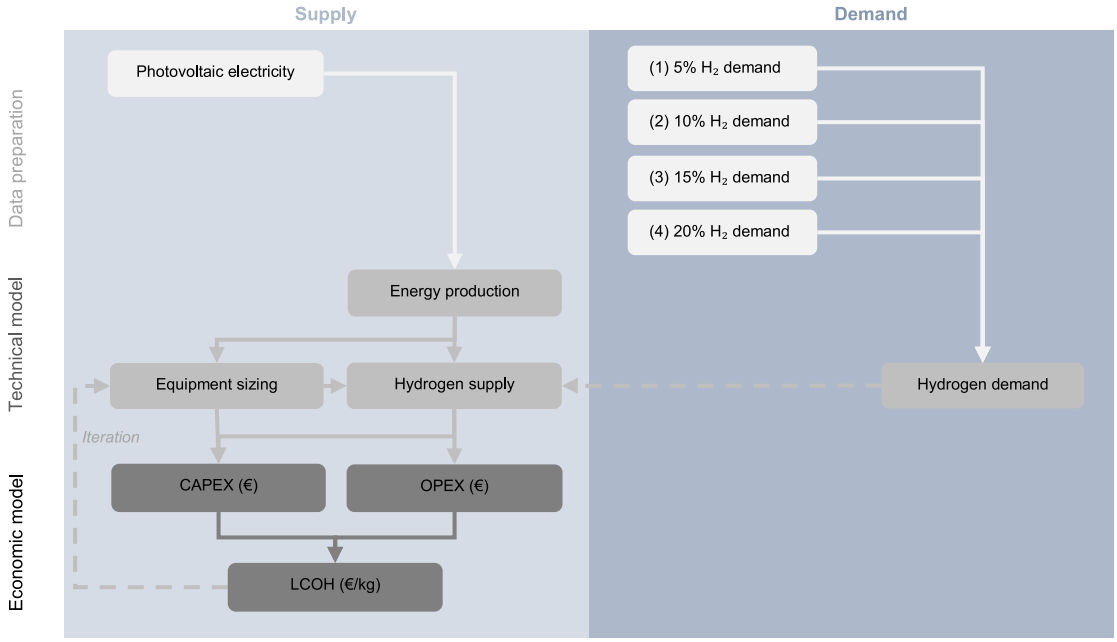

Fig. 4. Overall model to calculate the levelised cost of delivered hydrogen ($LCOH_D$) from a photovoltaic battery electrolyser system (PBES).

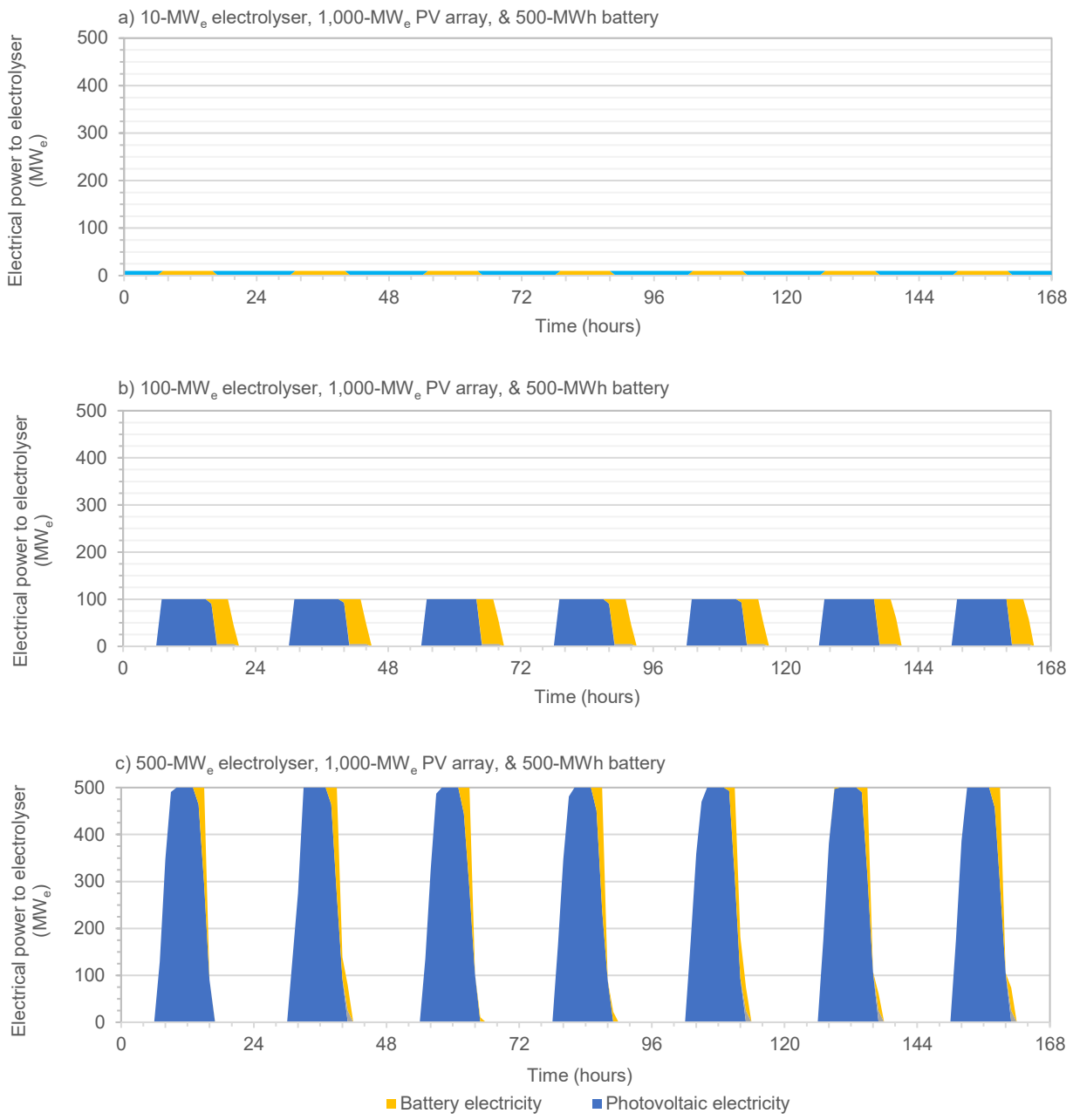

Fig. 5. Impact of electrolyser size (a) 10 MW_e, b) 100 MW_e and c) 500 MW_e on electrolyser operational hours for a 1,000-MW_e PV array and 500-MWh_e battery.

different equipment size configurations without considering the specifics of hydrogen demand. This enables a general understanding of system integration challenges and opportunities. The second part (sections 3.2, 3.3, and 3.4) presents the optimum equipment sizes to supply hydrogen that meet the demands for the hydrogen injection scenarios.

3.1. Impact of PV array, battery and electrolyser sizes on techno-economic performance

The selection of electrolyser size significantly impacts the techno-economic performances of the PBES. When a 1,000-MW_e PV array and a 500-MWh battery are coupled with a 10-MW_e electrolyser, the capacity factor of the electrolyser reaches 100%, as illustrated in Fig. 5.a for one week of electrolyser operation. However, 97% of the PV electricity is unable to be converted to hydrogen due to the small size of the electrolyser. For the grid-connected system, the unconverted PV electricity can be transferred to electricity grid to improve the revenue that aids the cost reduction, which otherwise becomes curtailed electricity. As a result, the $LCOH_D$ for this simplified case is very high at 25 €/kg. When the same sizes of PV arrays and battery are integrated with a 100-MW_e, there are some hours where the electrolyser cannot operate due to the absence of electricity supply from both PV and battery. Hence the capacity factor of the electrolyser is now 60%, as shown in Fig. 5.b. The surplus PV electricity and $LCOH_D$ are 76% and 5 €/kg, respectively. Fig. 5.c shows the electrolyser performance using the same sizes of PV array and battery with a 500-MW_e electrolyser. Even though the capacity factor of the electrolyser is only 35%, the $LCOH_D$ is calculated at 2.4 €/kg due to fact that 91% of the PV electricity can be used. Thus, the impact of reducing the surplus PV electricity to minimise $LCOH_D$ is larger than increasing the electrolyser's capacity factor.

To evaluate the impacts of different sizes of PV array and battery, Fig. 6a shows the $LCOH_D$ for 1,000-MW_e, 2,000-MW_e and 3,000-MW_e PV arrays, each of which is coupled with a 0-MWh 3,000-MWh or 6,000-MWh battery and compressed hydrogen storage with capacity of 5%

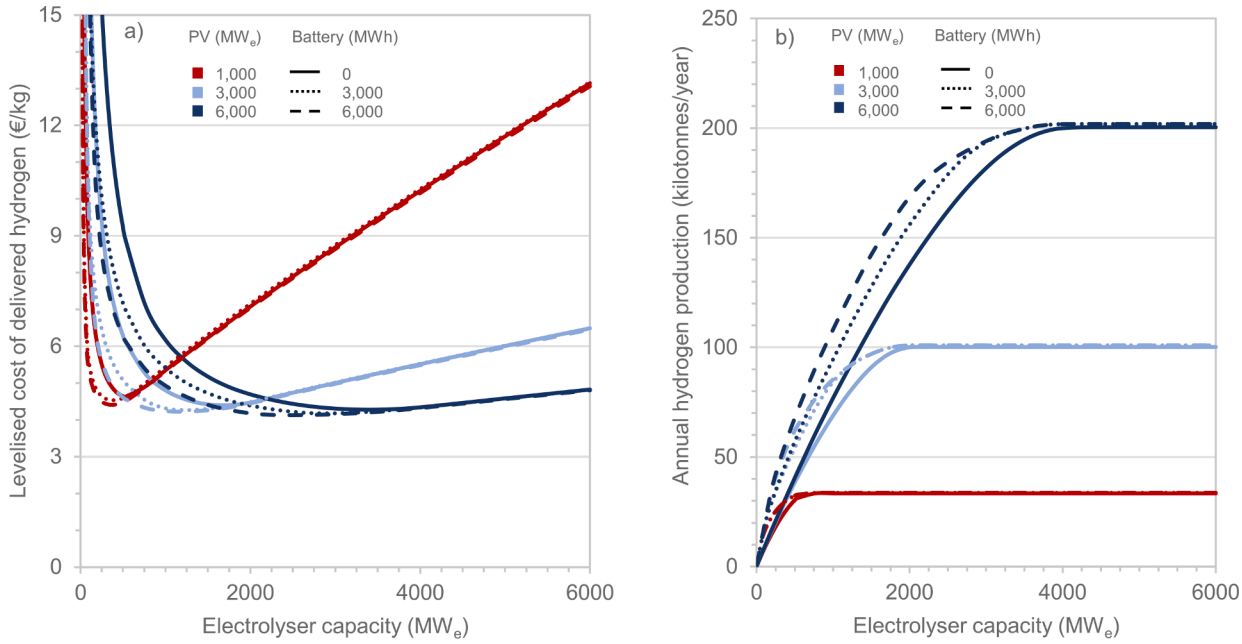

Fig. 6. Impact of the sizes of PV array, battery, and electrolyser on a) levelised cost of delivered hydrogen (€/kg) and b) annual hydrogen production (kilotonnes/year) at the photovoltaic battery electrolyser system with compressed hydrogen storage subsystem ($PBES_C$).

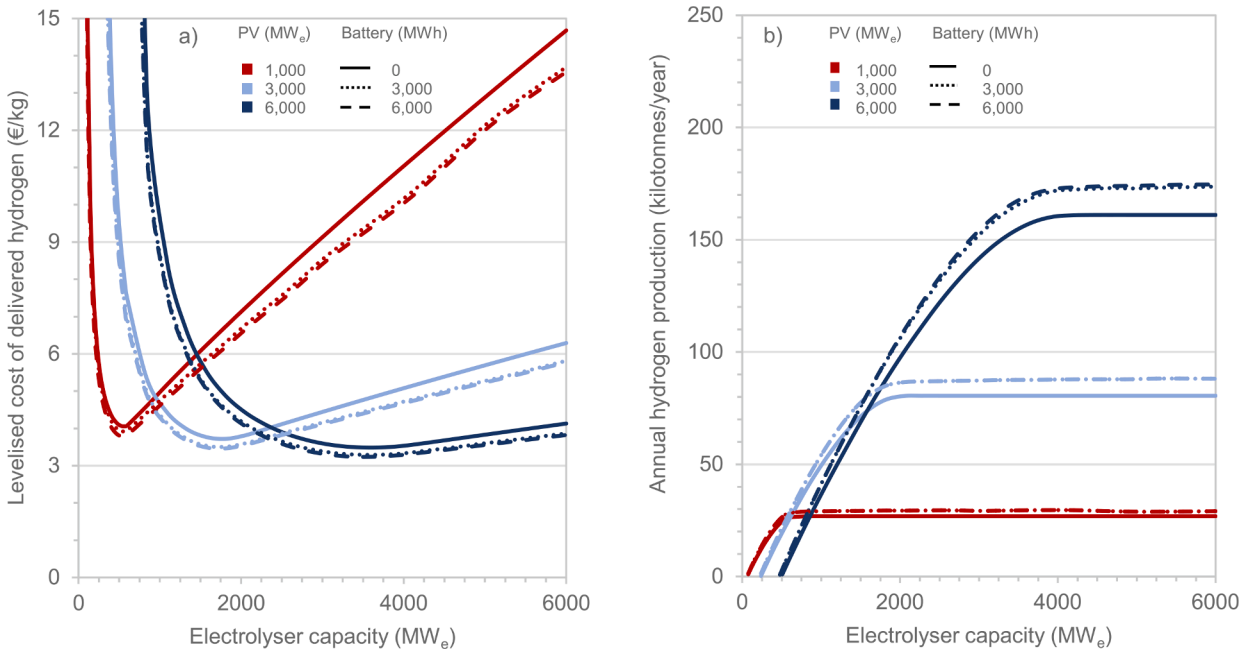

Fig. 7. Impact of the sizes of PV array, battery, and electrolyser on a) levelised cost of delivered hydrogen (€/kg) and b) annual hydrogen production (kilotonnes/year) at the photovoltaic battery electrolyser system with liquefied hydrogen storage subsystem ($PBES_L$).

of annual hydrogen production. The increase of PV and battery capacities results in the reduction of $LCOH_D$ for larger electrolysers due to the fact that more hydrogen is produced, as shown in Fig. 6.b. However, the $LCOH_D$ increases over the large electrolyser sizes due to capacity factor of electrolyser decreases. The impacts of different PV arrays, electrolyser, and battery sizes coupled with liquefied hydrogen storage (to accommodate 5% annual hydrogen production) on $LCOH_D$ and annual hydrogen production are shown in Fig. 7.a and Fig. 7.b, respectively. When there is no specific hydrogen demand needs to be addressed, it can be seen that the $LCOH_D$ can be significantly lower for liquefied storage than for compressed storage. However, the liquefied storage produces less hydrogen annually than compressed storage due to the energy-intensive liquefaction process, which diverts PV electricity from the electrolyser. At minimum $LCOH_D$, the capacity factors of electrolysers are 41% for compressed hydrogen and 26% for liquefied hydrogen.

3.2. Optimum equipment sizes for all scenarios

Minimum $LCOH_D$ to meet the hydrogen blending demand can be found using an optimum combination of PV, electrolyser, and battery sizes. The optimum electrolyser, PV array, and battery sizes to deliver to deliver 25.47 kilotonnes/ year or 5% hydrogen demand are 470 MWe,

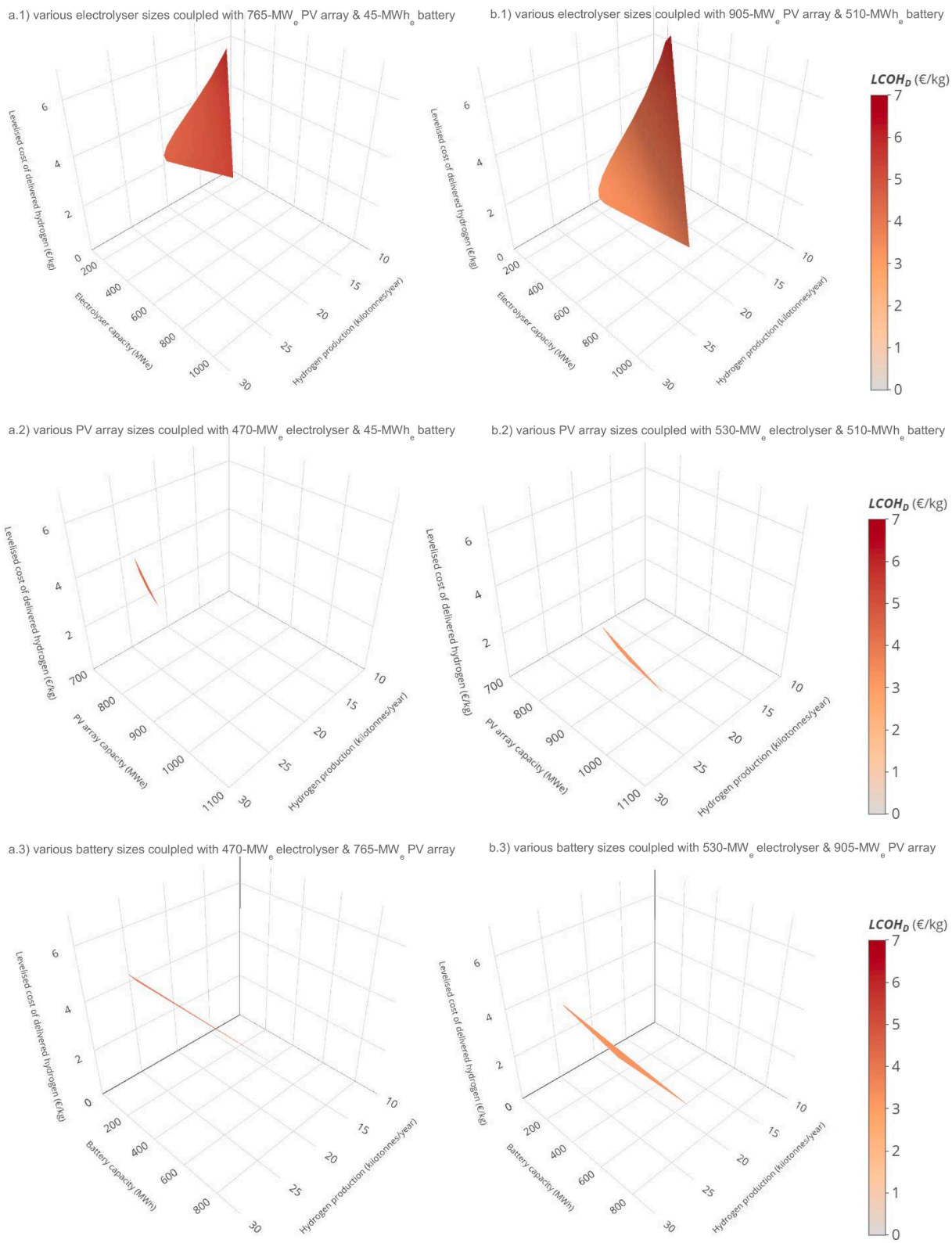

Fig. 8. A sample of equipment sizing of (a) photovoltaic battery electrolyser system with compressed ($PBES_C$) and (b) liquefied ($PBES_L$) hydrogen storage to deliver 25.47 kilotonnes/ year or 5% hydrogen demand at minimum levelised cost of delivered hydrogen ($LCOH_D$) by using (1) various electrolyser, (2) PV array, and (3) battery sizes.

765 MWe, and 45 MWh for gaseous storage, and 530 MWe, 905 MWe, and 510 MWh for liquid storage, respectively. Fig. 8 shows the impact of varying sizes for one equipment while maintaining the rest of equipment with its optimum sizes. It can be seen that electrolyser sizes have the significant impacts to both $LCOH_D$ and hydrogen production, especially or liquid storage system. However, modifying both PV array and battery sizes have the low impacts to $LCOH_D$ but hydrogen production. Therefore, beyond these optimum sizes, hydrogen production does not meet

Table 5
Summary of the optimum equipment sizes for all scenarios.

Parameters	Unit	Demand scenarios			
		5%	10%	15%	20%
H_2 demand	kilotonnes/year	25.47	50.41	77.29	106.24
Photovoltaic battery electrolyser system with compressed ($PBES_C$) hydrogen storage					
$LCOH_D$	€/kg	3.84	3.78	3.73	3.69
Photovoltaic array size	MW_e	765	1,515	2,325	3,195
Electrolyser size	MW_e	470	930	1,425	1,955
Battery size	MWh	45	85	115	180
Storage size (H_2 mass)	Kilotonnes	1.44	2.84	4.35	5.97
Storage size (H_2 volume)	m^3	70,158	138,414	211,608	290,843
Photovoltaic battery electrolyser system with liquefied ($PBES_L$) hydrogen storage					
$LCOH_D$	€/kg	3.23	3.04	2.91	2.81
Photovoltaic array size	MW_e	905	1,790	2,720	3,735
Electrolyser size	MW_e	530	1,070	1,690	2,340
Battery size	MWh	510	1,070	1,560	2,140
Storage size (H_2 mass)	Kilotonnes	1.33	2.90	4.47	6.22
Storage size (H_2 volume)	m^3	18,671	40,916	63,034	87,675

demand at minimum $LCOH_D$. The $LCOH_D$ to deliver the 5% to 20% hydrogen volume fraction are in the range of 3.69 to 3.84 €/kg for $PBES_C$ and 2.81 to 3.23 €/kg for $PBES_L$. The optimum equipment sizes to meet other hydrogen demands at minimum $LCOH_D$ are found iteratively and listed in Table 5.

The large sizes of hydrogen storage required in this study are due to the need to meet hydrogen demand targets throughout the whole year, which implies a need for seasonal storage. Vast land area is needed by $PBES_C$ for the buried pipes. In contrast, the high volumetric density of liquified hydrogen at $PBES_L$ reduces the required areas to about one third of buried pipe sizes. To supply hydrogen demand for the 20% blend scenario, the $PBES_L$ needs spherical tanks with a total capacity of 6,222 tonnes. The current largest spherical tank that stores liquified hydrogen (270 tonnes or 3,800 m^3) can be found in the National Aeronautics and Space Administration (NASA) at the Kennedy Space Center in Florida [34]. The battery size for the liquid hydrogen system is approximately 12 times larger than that required for a similarly-sized compressed hydrogen system, due to the requirement to power the liquefaction unit at night. The capacity factor of electrolyser for $PBES_C$ and $PBES_L$ are between 26% and 30% for all scenarios. The surplus of photovoltaic electricity is less than 2% for all systems.

Fig. 9 shows the comparison of the $LCOH_D$ and its contributors for each of the optimum configurations. It can be seen that storing large quantities of gaseous hydrogen leads to higher $LCOH_D$ than one that stores liquid hydrogen, even though the cost contribution of PV arrays increases due to the additional elelctricity demand for liquefaction. For compressed hydrogen, the costs of buried pipes are one of the main expenses and not significantly impacted by economies of scale due or technological learning. For a similar scale of hydrogen storage capacity (tonnes), liquid hydrogen offers lower capital costs compared to compressed storage. The larger share of battery costs for liquid hydrogen compared to compressed hydrogen also benefits liquid hydrogen to further reduce $LCOH_D$ when more hydrogen is injected (e.g. for 20% compared to 5% hydrogen demand). This is due to a large battery for large hydrogen demand bringing an advantage to the economies of scale.

3.3. Hydrogen supply from optimally sized equipment

Fig. 10 shows the one-week hydrogen supply perfromance of the $PBES_C$ for each blending scenario. The solid colours represent the hydrogen flow for grid injection, and pattern colours indicate the hydrogen flow to storage. The hydrogen flow for grid injection can be from storage (dark red) or from the electrolyser, powered by PV (yellow) or battery (blue). It can be seen that hydrogen production using direct PV electricity follows the solar energy profile during the day, with some additional hours of battery electricity afterwards. Part of the hydrogen produced during the day is kept in storage for supply during the absence of sunlight. Therefore, the $PBES_C$ can deliver the hourly hydrogen demand throughout the year. Fig. 11 shows the results for $PBES_L$ for the same one-week hydrogen supply perfromance. Even though the sizes of PV arrays for $PBES_L$ are larger than $PBES_C$, hydrogen production using direct PV electricity reduces since this electricity is used to supply the liquefaction process and charge much larger batteries. In addition, the battery in the $PBES_L$ provides more electricity for the electrolyser during

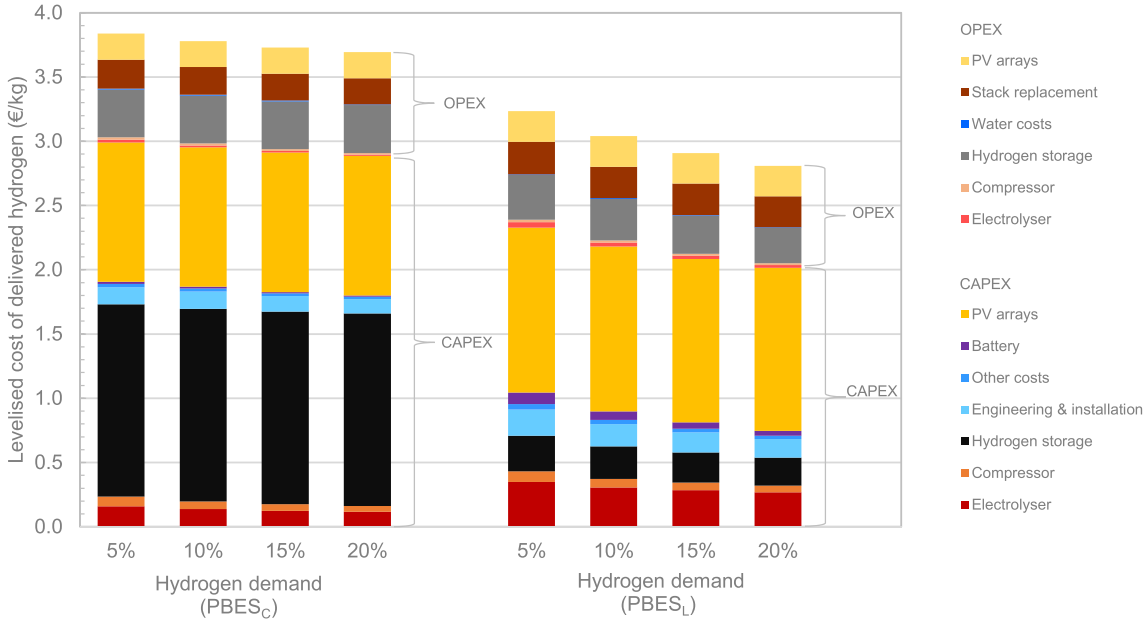

Fig. 9. The share of CAPEX and OPEX in $LCOH_D$ for the photovoltaic battery electrolyser system with compressed hydrogen storage subsystem ($PBES_C$) and with Liquefied Hydrogen Storage Subsystem ($PBES_L$).

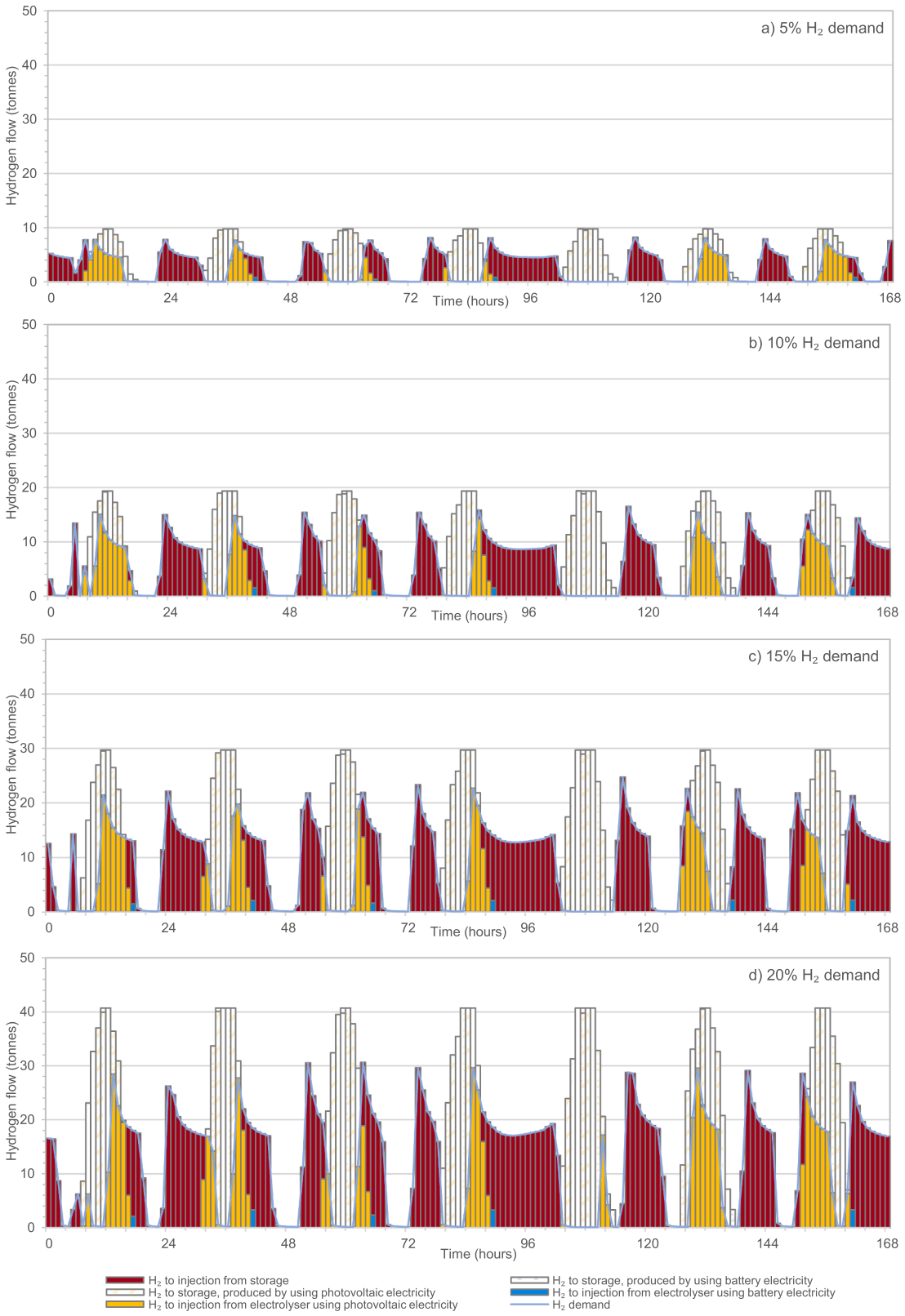

Fig. 10. Hourly hydrogen supply performance for one week of operation for all hydrogen demand scenarios with compressed hydrogen storage.

night than in thr $PBES_C$. The hydrogen storage performances of the $PBES_C$ and $PBES_L$ for all scenarios are illustrated in Fig. 12. It can be seen that the storage profiles for all scenarios are similar in that most surplus hydrogen is produced and stored during summer and released during winter.

3.4. Energy and water intensities of hydrogen supply

The overall energy efficiency of converting PV electricity to compressed hydrogen gas for blending in natural gas transmission are 67% for $PBES_C$ and 56% $PBES_L$, using the lower heating value of hydrogen

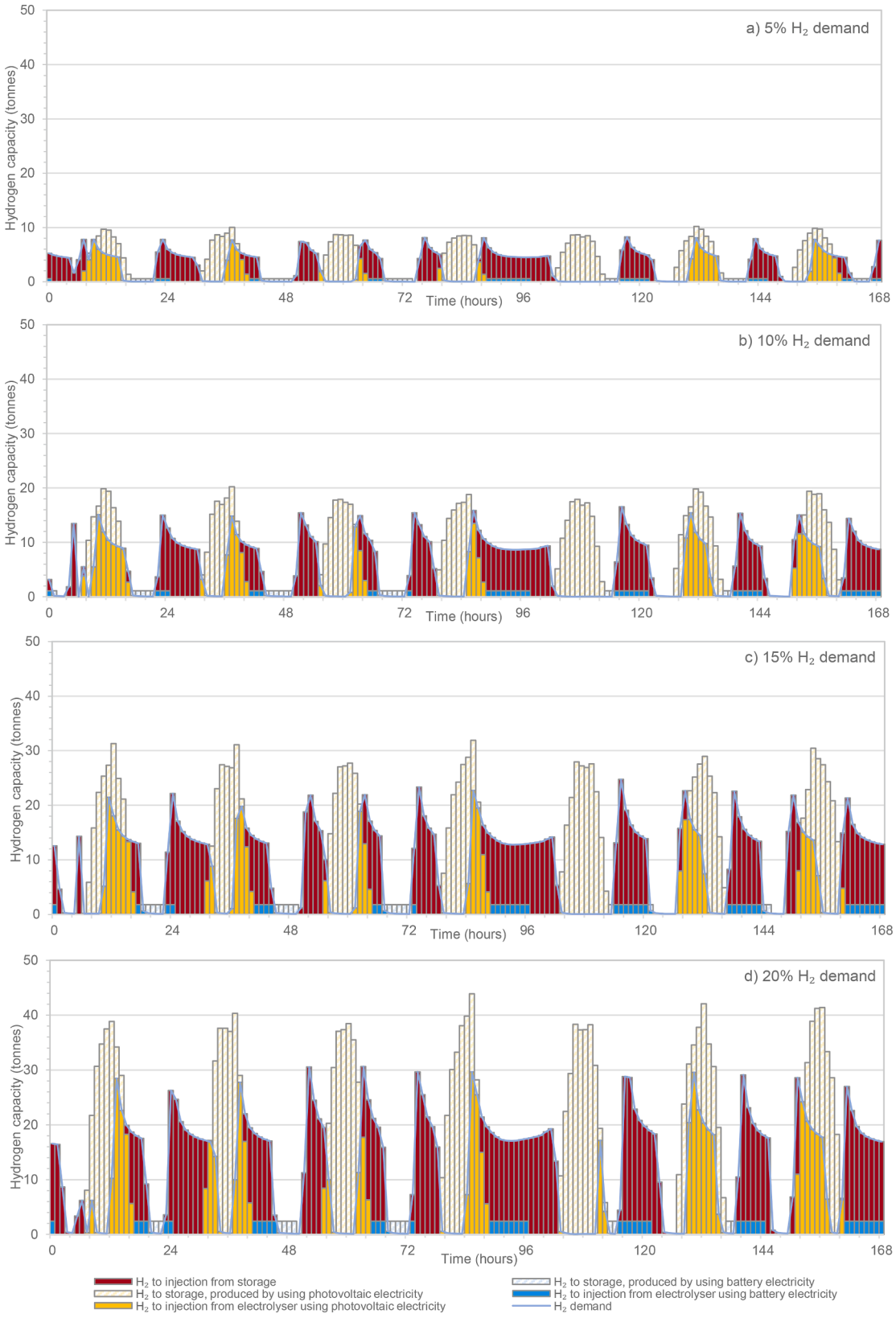

Fig. 11. Hourly hydrogen supply performance for one week of operation for all hydrogen demand scenarios with liquefied hydrogen storage.

(LHV_{H2}). For what concerns the transport in blended form, the energy cost increase at the compressor unit ranges from about +9% for the 5% blend scenario to about +32% for the 20% scenario. However, it negligibly affect the overall transport efficiency of the high pressure natural gas pipeline system, that is 99.4% in the 5% scenario and 99.3% in the 20% scenario (in the reference case with 100% natural gas transport it is 99.5%) [50]. The shares of energy for hydrogen production in the compressed (and liquefied) configurations to meet 5%

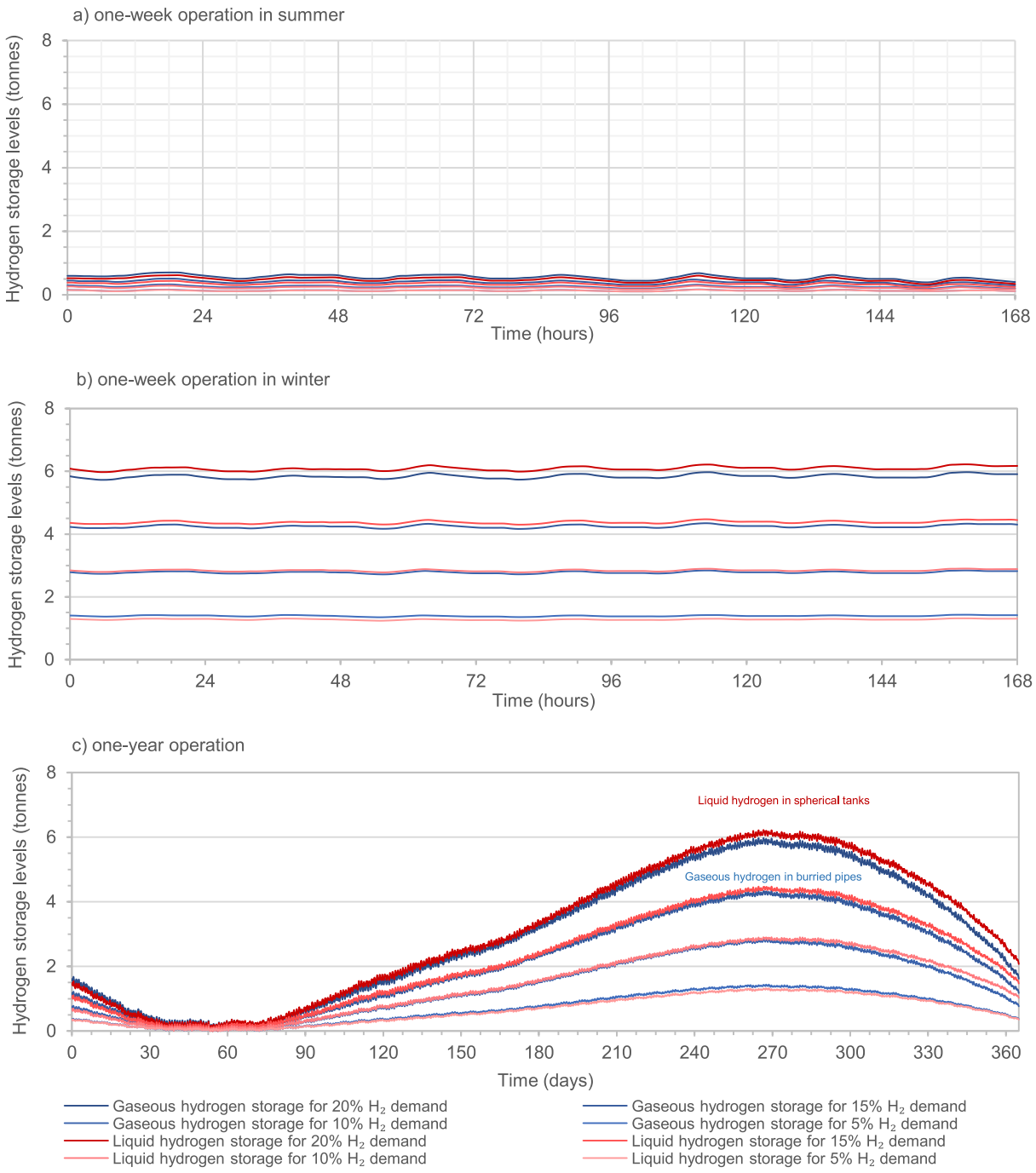

Fig. 12. Hydrogen storage profiles for all hydrogen demand scenarios by the photovoltaic battery electrolyser system with compressed ($PBES_C$) and liquefied hydrogen storages ($PBES_L$) for a) one-week operation in summer, b) one-week operation in winter, and c) one-year operation.

hydrogen demand are 98.5% (82.7%) for electrolysis, 1.4% (1.2%) for compression, and 0.06% (0.05%) for desalination. As described in subsection 2.6., the desalination system is not included in the PBES. The liquefied configuration additionally requires 16% for the liquefaction unit. Thus, the total energy intensity of hydrogen production is in the range 49–58 kWh/kg for all hydrogen demand scenarios. The average water intensity of hydrogen production is 15 l/kg, meaning that the PBES requires 0.4 to 1.7 million m^3 per year to meet hydrogen demand for the 5% to 20% injection scenarios.

3.5. Sensitivity analysis

The sensitive variables are evaluated for (1) technical parameters (efficiencies of PV, electrolyser, battery, and specific energy consumption of liquefaction unit), and (2) economic parameters (capital costs of PV, electrolyser, battery, and storage). The impact on $LCOH_D$ in percentage can be evaluated by changing the parameters' values by 10% and + 10% of initial values as shown in Fig. 13. On the technical side, the PV and electrolyser efficiencies significantly impact $LCOH_D$ in both gaseous and liquid systems. On the economic side, PV capital cost is the most sensitive parameter for a liquid system. In comparison, in addition

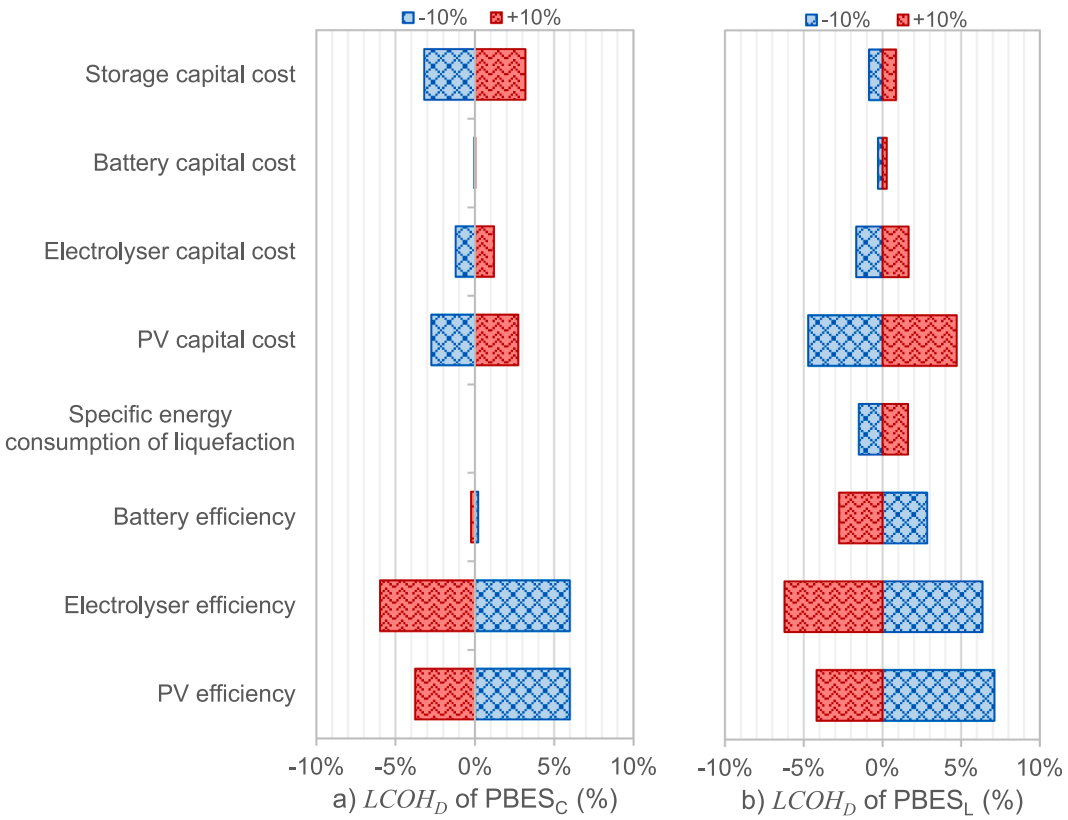

Fig. 13. Sensitivity analysis for technical and economic parameters for the photovoltaic battery electrolyser system (a) with compressed hydrogen storage subsystem (PBESC) and (b) with Liquefied Hydrogen Storage Subsystem ($PBES_L$).

to PV capital cost, storage capital cost is also impactful to $LCOH_D$ of the gaseous system.

4. Conclusions

A techno-economic model of hydrogen production in a photovoltaic battery electrolyser system (PBES) for injection and blending into a natural gas transmission pipeline was performed in this study. Mellitah in Libya is selected as the location for this case study. The PBES includes a polycrystalline silicon photovoltaic (PV) array to generate electricity, a lithium-ion battery to temporarily store PV electricity, an alkaline water electrolyser to produce hydrogen, a reciprocating compressor to compress the hydrogen to 80 barg, and large-scale gaseous or liquid hydrogen storage to maintain the flow rate of hydrogen required for constant volume fraction in the range 5–20% in the Green Stream gas pipeline to Italy. Hourly PV electricity output is simulated using the European Union Photovoltaic Geographical Information System (EU-PVGIS). The levelised cost of delivered hydrogen ($LCOH_D$) and hydrogen blending demand are used as the key parameters to optimise the size of components in the PBES.

Results show the selection of PV, electrolyser and battery sizes can significantly impact the techno-economic performance of the PBES, as indicated by $LCOH_D$. The optimum equipment sizes of PBES are selected to deliver minimum $LCOH_D$ while meeting hydrogen demand. The $LCOH_D$ and hydrogen production capacity from the optimum systems to meet the 5%, 10%, 15% and 20% hydrogen blending demands are in the range of 3.69 to 3.84 €/kg when coupled with compressed hydrogen storage subsystem ($PBES_C$) and 2.81 to 3.23 €/kg when coupled with liquefied hydrogen storage subsystem ($PBES_L$). In terms of mass, the largest storage capacity required for either compressed or liquefied hydrogen is around 6 kilotonnes. In terms of volume, the compressed hydrogen storages require the significant volumes between 70 and 290 thousand m^3. In contrast, liquefaction process of $PBES_L$ reduces the required volumes to between 18 and 87 thousand m^3. The large sizes of hydrogen storage in this study are due to the fact that most of the storable hydrogen is produced in summer to meet the annual demand for hydrogen blending.

Future studies could explore the addition of wind and/or concentrated solar power (CSP) for hydrogen production. Alternative large-scale storages of hydrogen for long-distance transmission is necessary to investigate. These could include compressed hydrogen gas storage at salt caverns and depleted natural gas reservoirs. Future work could also seek to integrate PBES with desalination powered by either CSP or direct solar energy. On the demand side, two potential avenues of future work present themselves. One involves allowing blending volume fractions to float within a range (for example 7.5%-12.5% instead of exactly 10%), which could enable smaller equipment and higher capacity factors. The other avenue would explore PBES configuration for 100% hydrogen injection.

CRediT authorship contribution statement

Tubagus Aryandi Gunawan: Conceptualization, Methodology, Validation, Investigation, Data curation, Formal analysis, Writing – original draft, Visualization. **Marco Cavana:** Conceptualization, Investigation, Data curation, Writing – review & editing. **Pierluigi Leone:** Conceptualization, Investigation, Writing – review & editing, Supervision, Project administration, Funding acquisition. **Rory F.D. Monaghan:** Conceptualization, Investigation, Writing – review & editing, Supervision, Project administration, Funding acquisition.

Declaration of Competing Interest

The authors declare the following financial interests/personal relationships which may be considered as potential competing interests: Tubagus Aryandi Gunawan reports financial support was provided by EU Interreg North-West Europe programme. Rory F.D. Monaghan reports financial support was provided by EU Interreg North-West Europe programme. Tubagus Aryandi Gunawan reports financial support was provided by Sustainable Energy Authority of Ireland. Rory F.D. Monaghan reports financial support was provided by Sustainable Energy Authority of Ireland. Marco Cavana reports financial support was provided by European Education and Culture Executive Agency. Pierluigi Leone reports financial support was provided by European Education and Culture Executive Agency. Rory F.D. Monaghan reports a relationship with EU Interreg North-West Europe programme that includes: funding grants. Pierluigi Leone reports a relationship with European Education and Culture Executive Agency that includes: funding grants.

Data availability

Data will be made available on request.

Acknowledgement

The authors gratefully acknowledge the funding support from the EU Interreg North-West Europe programme through the GENerating energy secure COMMunities through smart renewable hydrogen (GENCOMM) project (grant number NWE 334) and the Sustainable Energy Authority of Ireland (SEAI) RDD Programme (grant number RDD 445).

The authors wish also to thank the European Education and Culture Executive Agency for funding the Enbrain project, in the framework of the Erasmus + CBHE programm, aiming at starting a master in renewable and sustainable energy in five Libyan univerties, and from which the interest in a case study about Libya partially originated.

References

[1] European Comission. A hydrogen strategy for a climate-neutral Europe. Brussels, Belgium. 2020; 2020.
[2] van Wijk PA, Wouters F. A North Africa - Europe Hydrogen Manifesto. London, UK. 2019; 2019. [Online]. Available: https://www.middleeast-energy.com/content/dam/Informa/Middle-East-Electricity/middle-east-energy-2021/reports—external/Dii hydrogen study (November 2019)_print.pdf.
[3] European Commission. Quarterly Report on European Gas Markets (Q1 to Q4 in 2019). Brussels, Belgium. 2019; 2019.
[4] Renewable Power Generation Costs | IRENA, Renewable Power Generation Costs in 2020; 2020. [Online]. Available: https://www.irena.org/-/media/Files/IRENA/Agency/Publication/2018/Jan/IRENA_2017_Power_Costs_2018.pdf.
[5] International Renewable Energy Agency - IRENA, Future of solar photovoltaic, vol. November. Abu Dhabi, UEA. 2019.; 2019. [Online]. Available: https://www.irena.org/-/media/Files/IRENA/Agency/Publication/2019/Oct/IRENA_Future_of_wind_2019.pdf.
[6] Zhou Y, Gu A. Learning curve analysis of wind power and photovoltaics technology in US: Cost reduction and the importance of research, development and demonstration. Sustainability (Switzerland) 2019;11(8):pp. https://doi.org/10.3390/su11082310.
[7] Mallapragada DS, Pilas DD, Fernandez PG. System implications of continued cost declines for wind and solar on driving power sector decarbonization. Cambridge, USA: MIT Energy Initiative; 2020, 2020..
[8] Kikuchi Y, Ichikawa T, Sugiyama M, Koyama M. Battery-assisted low-cost hydrogen production from solar energy: Rational target setting for future technology systems. Int J Hydrogen Energy 2019;44(3):1451–65. https://doi.org/10.1016/j.ijhydene.2018.11.119.
[9] Hemmati R, Mehrjerdi H, Bornapour M. Hybrid hydrogen-battery storage to smooth solar energy volatility and energy arbitrage considering uncertain electrical-thermal loads. Renew Energy Jul. 2020;154:1180–7. https://doi.org/10.1016/j.renene.2020.03.092.
[10] Burhan M, Chua KJE, Ng KC. Sunlight to hydrogen conversion: Design optimization and energy management of concentrated photovoltaic (CPV-Hydrogen) system using micro genetic algorithm. Energy Mar. 2016;99:115–28. https://doi.org/10.1016/j.energy.2016.01.048.
[11] Castañeda M, Cano A, Jurado F, Sánchez H, Fernández LM. Sizing optimization, dynamic modeling and energy management strategies of a stand-alone PV/hydrogen/battery-based hybrid system. Int J Hydrogen Energy Apr. 2013;38(10):3830–45. https://doi.org/10.1016/j.ijhydene.2013.01.080.
[12] Xie Y, Ueda Y, Sugiyama M. Greedy energy management strategy and sizing method for a stand-alone microgrid with hydrogen storage. J Energy Storage Dec. 2021;44. https://doi.org/10.1016/j.est.2021.103406.
[13] Marocco P, Ferrero D, Lanzini A, Santarelli M. Optimal design of stand-alone solutions based on RES + hydrogen storage feeding off-grid communities. Energy Convers Manag Jun. 2021;238. https://doi.org/10.1016/j.enconman.2021.114147.
[14] Mah AXY, et al. Optimization of a standalone photovoltaic-based microgrid with electrical and hydrogen loads. Energy Nov. 2021;235. https://doi.org/10.1016/j.energy.2021.121218.
[15] Dispenza G, Sergi F, Napoli G, Antonucci V, Andaloro L. Evaluation of hydrogen production cost in different real case studies. J Energy Storage 2019;vol. 24, no. April:100757. https://doi.org/10.1016/j.est.2019.100757.
[16] Coppitters D, de Paepe W, Contino F. Robust design optimization and stochastic performance analysis of a grid-connected photovoltaic system with battery storage and hydrogen storage. Energy Dec. 2020;213. https://doi.org/10.1016/j.energy.2020.118798.
[17] Cerchio M, Gullí F, Repetto M, Sanfilippo A. Hybrid energy network management: Simulation and optimisation of large scale PV coupled with hydrogen generation. Electronics (Switzerland) Oct. 2020;9(10):1–17. https://doi.org/10.3390/electronics9101734.
[18] Zhang Y, Campana PE, Lundblad A, Yan J. Comparative study of hydrogen storage and battery storage in grid connected photovoltaic system: Storage sizing and rule-based operation. Appl Energy 2017;201:397–411. https://doi.org/10.1016/j.apenergy.2017.03.123.
[19] Andersson J, Grönkvist S. Large-scale storage of hydrogen. Int J Hydrogen Energy Elsevier Ltd, May 03, 2019;44(23):11901–19. doi: 10.1016/j.ijhydene.2019.03.063.
[20] Kavadias KA, Apostolou D, Kaldellis JK. Modelling and optimisation of a hydrogen-based energy storage system in an autonomous electrical network. Appl Energy 2018;227(January 2017):574–86. doi: 10.1016/j.apenergy.2017.08.050.
[21] Farag HEZ, Al-Obaidi A, Khani H, El-Taweel N, El-Saadany EF, Zeineldin HH. Optimal operation management of distributed and centralized electrolysis-based hydrogen generation and storage systems. Electr Power Syst Res Oct. 2020;187. https://doi.org/10.1016/j.epsr.2020.106476.
[22] Bünger U, Michalski J, Crotogino F, Kruck O. Large-scale underground storage of hydrogen for the grid integration of renewable energy and other applications. In: Compendium of Hydrogen Energy. Elsevier; 2016. p. 133–63. https://doi.org/10.1016/b978-1-78242-364-5.00007-5.
[23] López E, Isorna F, Rosa F. Optimization of a solar hydrogen storage system: Exergetic considerations. Int J Hydrogen Energy Jul. 2007;32(10–11):1537–41. https://doi.org/10.1016/j.ijhydene.2006.10.032.
[24] Mallapragada DS, Gençer E, Insinger P, Keith DW, O'Sullivan FM. Can Industrial-Scale Solar Hydrogen Supplied from Commodity Technologies Be Cost Competitive by 2030? Cell Rep Phys Sci 2020;1(9):pp. https://doi.org/10.1016/j.xcrp.2020.100174.
[25] Welder L, Ryberg DS, Kotzur L, Grube T, Robinius M, Stolten D. Spatio-temporal optimization of a future energy system for power-to-hydrogen applications in Germany. Energy Sep. 2018;158:1130–49. https://doi.org/10.1016/j.energy.2018.05.059.
[26] Emonts B, et al. Flexible sector coupling with hydrogen: A climate-friendly fuel supply for road transport. Int J Hydrogen Energy 2019;44(26):12918–30. https://doi.org/10.1016/j.ijhydene.2019.03.183.
[27] Mah AXY, et al. Spatial optimization of photovoltaic-based hydrogen-electricity supply chain through an integrated geographical information system and mathematical modeling approach. Clean Technol Environ Policy Jan. 2022;24(1):393–412. https://doi.org/10.1007/s10098-021-02235-4.
[28] Elberry AM, Thakur J, Veysey J. Seasonal hydrogen storage for sustainable renewable energy integration in the electricity sector: A case study of Finland. J Energy Storage Dec. 2021;44. https://doi.org/10.1016/j.est.2021.103474.
[29] O'Dwyer C, Dillon J, O'Donnell T. Long-Term Hydrogen Storage—A Case Study Exploring Pathways and Investments. Energies (Basel) Feb. 2022;15(3). doi: 10.3390/en15030869.
[30] Samsatli S, Samsatli NJ. The role of renewable hydrogen and inter-seasonal storage in decarbonising heat – Comprehensive optimisation of future renewable energy value chains. Appl Energy Jan. 2019;233–234:854–93. https://doi.org/10.1016/j.apenergy.2018.09.159.
[31] Quarton CJ, Samsatli S. Should we inject hydrogen into gas grids? Practicalities and whole-system value chain optimisation. Appl Energy Oct. 2020;275. https://doi.org/10.1016/j.apenergy.2020.115172.
[32] Seo SK, Yun DY, Lee CJ. Design and optimization of a hydrogen supply chain using a centralized storage model. Appl Energy Mar. 2020;262. https://doi.org/10.1016/j.apenergy.2019.114452.
[33] Gabrielli P, Poluzzi A, Kramer GJ, Spiers C, Mazzotti M, Gazzani M. Seasonal energy storage for zero-emissions multi-energy systems via underground hydrogen storage. Renew Sustain Energy Rev Apr. 2020;121. https://doi.org/10.1016/j.rser.2019.109629.
[34] Bonadio L. Liquid. In: Encyclopedia of Electrochemical Power Sources, Amsterdam, the Netherlands; 2009. p. 421–39. doi: https://doi.org/10.1016/B978-044452745-5.00323-3.
[35] Aasadnia M, Mehrpooya M. Large-scale liquid hydrogen production methods and approaches: A review. Appl Energy Elsevier Ltd, Feb. 15, 2018;212:57–83. doi: 10.1016/j.apenergy.2017.12.033.
[36] Ghorbani B, Mehrpooya M, Aasadnia M, Niasar MS. Hydrogen liquefaction process using solar energy and organic Rankine cycle power system. J Clean Prod Oct. 2019;235:1465–82. https://doi.org/10.1016/j.jclepro.2019.06.227.

[37] Cardella U, Decker L, Klein H. Roadmap to economically viable hydrogen liquefaction. Int J Hydrogen Energy May 2017;42(19):13329–38. https://doi.org/10.1016/j.ijhydene.2017.01.068.
[38] Cardella U, Decker L, Sundberg J, Klein H. Process optimization for large-scale hydrogen liquefaction. Int J Hydrogen Energy Apr. 2017;42(17):12339–54. https://doi.org/10.1016/j.ijhydene.2017.03.167.
[39] Saadi FH, Lewis NS, McFarland EW. Relative costs of transporting electrical and chemical energy. Energy Environ Sci Mar. 2018;11(3):469–75. https://doi.org/10.1039/c7ee01987d.
[40] Miao B, Giordano L, Chan SH. Long-distance renewable hydrogen transmission via cables and pipelines. Int J Hydrogen Energy May 2021;46(36):18699–718. https://doi.org/10.1016/j.ijhydene.2021.03.067.
[41] Demir ME, Dincer I. Cost assessment and evaluation of various hydrogen delivery scenarios. Int J Hydrogen Energy May 2018;43(22):10420–30. https://doi.org/10.1016/j.ijhydene.2017.08.002.
[42] Wulf C, et al. Life Cycle Assessment of hydrogen transport and distribution options. J Clean Prod Oct. 2018;199:431–43. https://doi.org/10.1016/j.jclepro.2018.07.180.
[43] Reuß M, Grube T, Robinius M, Stolten D. A hydrogen supply chain with spatial resolution: Comparative analysis of infrastructure technologies in Germany. Appl Energy 2019;247(no. December 2018):438–53. doi: 10.1016/j.apenergy.2019.04.064.
[44] Liu J, Teng L, Liu B, Han P, Li W. Analysis of Hydrogen Gas Injection at Various Compositions in an Existing Natural Gas Pipeline. Front Energy Res Jul. 2021;9. https://doi.org/10.3389/fenrg.2021.685079.
[45] Influences of Hydrogen Blending on the Joule–Thomson Coefficient of Natural Gas.
[46] Pellegrino S, Lanzini A, Leone P. Greening the gas network – The need for modelling the distributed injection of alternative fuels. Renew Sustainable Energy Rev Elsevier Ltd, Apr. 01, 2017;70:266–86. doi: 10.1016/j.rser.2016.11.243.
[47] Mukherjee U, Elsholkami M, Walker S, Fowler M, Elkamel A, Hajimiragha A. Optimal sizing of an electrolytic hydrogen production system using an existing natural gas infrastructure. Int J Hydrogen Energy Aug. 2015;40(31):9760–72. https://doi.org/10.1016/j.ijhydene.2015.05.102.
[48] Gunawan TA, Singlitico A, Blount P, Burchill J, Carton JG, Monaghan RFD. At What Cost Can Renewable Hydrogen Offset Fossil Fuel Use in Ireland's Gas Network? Energies (Basel) Apr. 2020;13(7):1798. https://doi.org/10.3390/en13071798.
[49] Cavana M, Leone P. Solar hydrogen from North Africa to Europe through greenstream: A simulation-based analysis of blending scenarios and production plant sizing. Int J Hydrogen Energy 2021;46(43):22618–37. https://doi.org/10.1016/j.ijhydene.2021.04.065.
[50] Open Infrastructure Map. https://openinframap.org/#5.87/35.389/16.483/L,O (accessed Nov. 27, 2021).
[51] Joint Research Centre (JRC) EU Science Hub, EU Photovoltaic Geographical Information System (PVGIS): PV Performance tool. https://re.jrc.ec.europa.eu/pvg_tools/en/#PVP (accessed Mar. 14, 2021).
[52] Amos WA. Costs of Storing and Transporting Hydrogen, Report Number: NREL/TP-570-25106. Colorado, USA. 1998; 1998. [Online]. Available: http://www.doe.gov/bridge/home.html.
[53] Donadei S, Schneider GS. Compressed Air Energy Storage in Underground Formations. Elsevier Inc.; 2016. doi: 10.1016/B978-0-12-803440-8.00006-3.
[54] Aghahosseini A, Breyer C. Assessment of geological resource potential for compressed air energy storage in global electricity supply. Energy Convers Manag Aug. 2018;169:161–73. https://doi.org/10.1016/j.enconman.2018.05.058.
[55] Argonne National Laboratory. Overview of Interstate Hydrogen Pipeline Systems Environmental Science Division. ANL/EVS/TM/08-2. Argonne, Illinois; 2007. [Online]. Available: www.anl.gov.
[56] European Energy Research Alliance. Key Performance Indicators (KPIs) for FCH Research and Innovation, 2020 - 2030. Brussels, Belgium. 2020.; 2020.
[57] Stolzenburg K, Mubbala R. Integrated Design for Demonstration of Efficient Liquefaction of Hydrogen (IDEALHY) Fuel Cells and Hydrogen Joint Undertaking (FCH JU) Grant Agreement Number 278177 Title: Hydrogen Liquefaction Report; 2013.
[58] Syedt MT, Sherift SA, Veziroblu TN, Sheffield1 JW. An Economic Analysis Of Three Hydrogen Liquefaction Systems. ht. J Hydrogen Energy 1998;23(I):565–76.
[59] National Institute of Standards and Technology. Reference Fluid Thermodynamic and Transport Properties Database (REFPROP): Version 8.0. U.S. Department of Commerce. Gaithersburg, Maryland, US; 2020.
[60] Almaktar M, Elbreki AM, Shaaban M. Revitalizing operational reliability of the electrical energy system in Libya: Feasibility analysis of solar generation in local communities. J Clean Prod 2021;279:123647. https://doi.org/10.1016/j.jclepro.2020.123647.
[61] Glenk G, Reichelstein S. Economics of converting renewable power to hydrogen. Nat Energy 2019;4(3):216–22. https://doi.org/10.1038/s41560-019-0326-1.
[62] Buttler A, Spliethoff H. Current status of water electrolysis for energy storage, grid balancing and sector coupling via power-to-gas and power-to-liquids: A review. Renew Sustain Energy Rev 2018;82(2017):2440–54. https://doi.org/10.1016/j.rser.2017.09.003.
[63] Schmidt O, Gambhir A, Staffell I, Hawkes A, Nelson J, Few S. Future cost and performance of water electrolysis: An expert elicitation study. Int J Hydrogen Energy 2017;42(52):30470–92. https://doi.org/10.1016/j.ijhydene.2017.10.045.
[64] Mayer T, Semmel M, Guerrero Morales MA, Schmidt KM, Bauer A, Wind J. Techno-economic evaluation of hydrogen refueling stations with liquid or gaseous stored hydrogen. Int J Hydrogen Energy 2019;44(47):25809–33. https://doi.org/10.1016/j.ijhydene.2019.08.051.
[65] Apostolou D, Xydis G. A literature review on hydrogen refuelling stations and infrastructure. Current status and future prospects. Renew Sustain Energy Rev 2019;113(May 2018):109292. doi: 10.1016/j.rser.2019.109292.
[66] IRENA. Green Hydrogen Cost Reduction: Scaling up Electrolysers to Meet the 1.5°C Climate Goal. Abu Dhabi, UEA. 2020.; 2020. [Online]. Available: /publications/2020/Dec/Green-hydrogen-cost-reduction%0Ahttps://www.irena.org/-/media/Files/IRENA/Agency/Publication/2020/Dec/IRENA_Green_hydrogen_cost_2020.pdf.
[67] Tractebel E, Engie, Hinicio. Study on Early Business Cases for H2 in Energy Storage and More Broadly Power To H2 Applications. Brussels, Belgium; 2017. [Online]. Available: http://www.hinicio.com/inc/uploads/2017/07/P2H_Full_Study_FCHJU.pdf%0Ahttp://www.fch.europa.eu/sites/default/files/P2H_Full_Study_FCHJU.pdf%0Ahttp://www.hinicio.com/file/2018/06/P2H_Full_Study_FCHJU.pdf.
[68] Gökçek M, Kale C. Optimal design of a Hydrogen Refuelling Station (HRFS) powered by Hybrid Power System. Energy Convers Manag 2018;161(December 2017):215–24. doi: 10.1016/j.enconman.2018.02.007.
[69] Papadopoulos V, Desmet J, Knockaert J, Develder C. Improving the utilization factor of a PEM electrolyzer powered by a 15 MW PV park by combining wind power and battery storage – Feasibility study. Int J Hydrogen Energy 2018;43(34):16468–78. https://doi.org/10.1016/j.ijhydene.2018.07.069.
[70] Rowland L. 2020 Energy Storage Assessment Study: Black Hills Energy. Colorado, USA. 2020.; 2020.
[71] Ma T, Javed MS. Integrated sizing of hybrid PV-wind-battery system for remote island considering the saturation of each renewable energy resource. Energy Convers Manag 2019;182(December 2018):178–90. doi: 10.1016/j.enconman.2018.12.059.
[72] Song Z, Feng S, Zhang L, Hu Z, Hu X, Yao R. Economy analysis of second-life battery in wind power systems considering battery degradation in dynamic processes: Real case scenarios. Appl Energy 2019;vol. 251, no. March:113411. https://doi.org/10.1016/j.apenergy.2019.113411.
[73] World Bank. Renewable energy desalination: an emerging solution to close the water gap in MENA. Washington, DC, United States. 2012; 2013.
[74] Palenzuela P, Alarcón-Padilla DC, Zaragoza G. Large-scale solar desalination by combination with CSP: Techno-economic analysis of different options for the Mediterranean Sea and the Arabian Gulf. Desalination 2015;366:130–8. https://doi.org/10.1016/j.desal.2014.12.037.
[75] El-Bialy E, Shalaby SM, Kabeel AE, Fathy AM. Cost analysis for several solar desalination systems. Desalination 2016;384:12–30. https://doi.org/10.1016/j.desal.2016.01.028.
[76] Romeo LM, Cavana M, Bailera M, Leone P, Peña B, Lisbona P. Non-stoichiometric methanation as strategy to overcome the limitations of green hydrogen injection into the natural gas grid. Appl Energy Mar. 2022;309. https://doi.org/10.1016/j.apenergy.2021.118462.
[77] ENTSOG. ENTSOG Transparency Platform. https://transparency.entsog.eu/#/map, Jun. 25, 2022.